CHALMERS
UNIVERSITY OF TECHNOLOGY

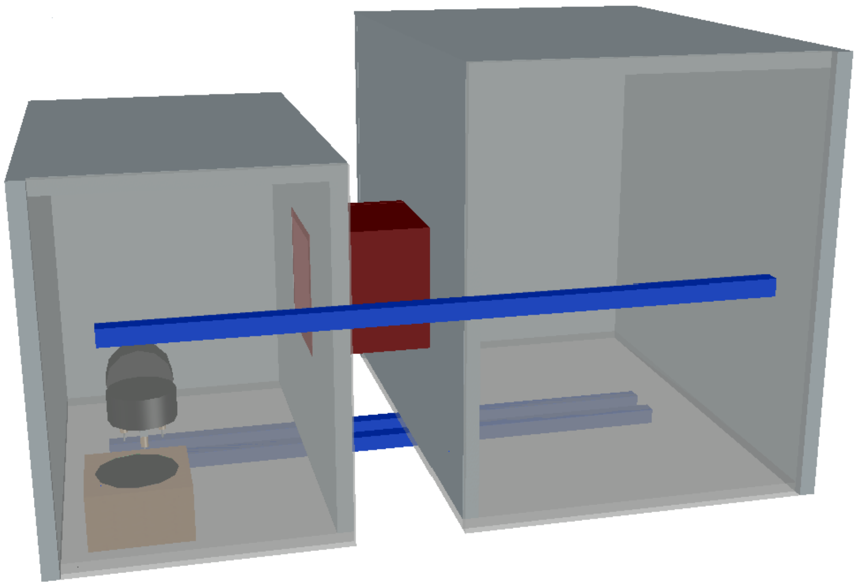

Investigations on operational transfer path analysis in combination with additional artificial excitation by the use of a physical model

Master's thesis in Sound and Vibration

LUCAS HEIDEMANN

Department of Architecture and Civil Engineering
CHALMERS UNIVERSITY OF TECHNOLOGY
Gothenburg, Sweden 2019

Master's thesis 2019: ACEX30 - 19 - 103

Investigations on operational transfer path analysis in combination with additional artificial excitation by the use of a physical model

LUCAS HEIDEMANN

Department of Architecture and Civil Engineering
Division of Applied Acoustics
Chalmers University of Technology
Gothenburg, Sweden 2019

Investigations on operational transfer path analysis in combination with additional artificial excitation by the use of a physical model
LUCAS HEIDEMANN

Supervisor: Otto Martner, Alex Sievi, Müller BBM GmbH
Examiner: Wolfgang Kropp, Division of Applied Acoustics,
Chalmers University of Technology

Master's Thesis 2019: ACEX30 - 19 - 103
Department of Architecture and Civil Engineering
Division of Applied Acoustics
Chalmers University of Technology
SE-412 96 Gothenburg
Telephone +46 31 772 1000

Cover: Drawing of the test setup.

Typeset in LaTeX
Gothenburg, Sweden 2019

Investigations on operational transfer path analysis in combination with additional artificial excitation by the use of a physical model
LUCAS HEIDEMANN
Division of Applied Acoustics
Department of Architecture and Civil Engineering
Chalmers University of Technology
Müller-BBM GmbH

Abstract

This thesis covers the influence on artificial excitation used together with operational data from an engine applied on operational transfer path analysis. Therefore, a physical model was built with two structure-borne sound paths and one airborne sound channel.

The history and theory of transfer path analysis is treated briefly and the setup of the model is explained. All paths of the model have been measured individually as well as combined to receive a basis to evaluate the transfer path synthesis results from both operational and combined operational and hammer data.

The crosstalk cancellation needed to receive the transmissibilities was performed with different data than the input signal of the synthesis. Three sets of impulse hammer measurements were used to see if artificial excitation is best to be performed before the source, at the interfaces or on the individual paths. All impulse hammer measurements were used for two different reference planes to derive measurement rules for combined measurements.

The results of the thesis indicate that impulse hammer measurements can be combined with operational data, if certain paths are calculated insufficiently. Therefore, every path has to be reached and hammer impacts have to be performed in all directions at or before the reference sensor. If the source is insufficient to excite all frequencies it can also help to excite the source itself with an impulse hammer.

Keywords: OTPA, Path Analysis, Physical model, TPS, CTC, Impulse hammer.

Contents

List of Figures

List of Tables

List of Abbreviations and conventions

Active part	Part of the system where the sources are located.
Answer	Point where the level of interest is measured and synthesized.
CTC	Cross-talk cancellation.
FFT	Fast Fourier Transform.
Interface	Connection between the active and passive part.
OTPA	Operational Transfer Path Analysis.
Passive part	Part of the system that gets excited by the active part. All answer points and usually also the references are located here.
PC	Principal components.
Reference	Measurement point on the transfer path used to calculate the Transmissibilities.
Reference plane	Plane in which all transmission paths are measured.
TPA	Transfer Path Analysis.
TPS	Transfer Path Synthesis.
Transfer function	Relation between input and output of a system.
Transmissibility	Relation between two outputs of a system.

1
Introduction

The Transfer Path Analysis (TPA) is a tool used in mainly the automotive sector of acoustics to describe the sound and vibration transmission from a sound source to a receiving point. This source can be for example mechanical noise produced by the motor or tires, electro-mechanical noise emitted by transformers or pressure changes in fluids or gases.

The noise is then transmitted through various paths to a receiving point, which is in TPA mostly called the answer point. This answer point is usually the sound pressure level at the driver's ears, but also vibrations of the steering wheel, the seat or the sound pressure level and vibration at any other position even outside the car can be chosen. Besides the automotive sector, TPA is also used for trains, ships, agricultural machinery and also sometimes in building acoustics. TPA can be used for trouble shooting, sound design and also as a step on the way to fulfil regulations.

Depending on the purpose of the TPA, different measures can be of interest. The first TPA measurements were performed to receive the operating forces of the source. Further developments were made that lead among others to the Transfer Path Synthesis (TPS), where the information gained from the analysis can be used to predict the sound with a different source, or to calculate the contribution of each path to the resulting sound pressure level at the answer point.

There are different approaches to obtain the transfer paths or transmissibilities between source and receiver. Best known is the Matrix Inversion (MI), also often referred to as traditional TPA. For this method, the sound source has to be removed and all coupling points have to be excited by either an impulse hammer or a shaker. The excitation force is then derived by the measured input force of the hammer, indicator accelerometers close to the mounting points and the measured sound pressure level or acceleration at the receiving position in both hammer measurements and measurements with the real source. This procedure has the advantage to result in a complex transfer function from each impact point to each answer point, a well known measure in all fields of acoustical engineering .

As this method can be very time consuming, further developments of the TPA were made in the last years. One of these developments is the Operational Transfer Path Analysis, OTPA. In the OTPA, transmissibilities are calculated from measurements with an operating real sound source like an engine. A transmissibility is not a relation between the input and the output of a system, but between two outputs. Among the advantages of this method, is that it leads to more realistic measurements, as the weight of the source can influence the paths, and saving of time, as the examined object can be used as it is. In operational measurements, all sensor positions are connected to each other via the object that should be measured. Therefore, all transfer functions are coupled and crosstalk occurs. To obtain linearly independent transfer functions, this crosstalk has to be cancelled. The crosstalk cancellation (CTC) needs varying input signals to calculate correct path contributions. These signals are usually reached by different operating conditions. While this can be easily reached in a car, a run up and a run down in different gears is sufficient, it can be difficult or impossible to have different operating conditions with other sound sources. For example a transformation unit in a train where the operational sound and vibration can not be changed easily can be hard to investigate with an OTPA. The excitation of the structure of interest to a singular point can also not be measured directly. Therefore the result of the CTC is usually called a set of transmissibilities.

An other limitation of the OTPA comes up if correlated signals are to be examined. This can happen if various electro-mechanical sources have the same function and are always operated together. If in the process of improving the sound transmission these sources have to be examined separately it may not be possible to distinguish the contribution of each source via OTPA.

1.1 Situation and task of the thesis

In OTPA measurements it is usually assumed that the signal of the source is sufficient to excite all frequencies of interest. If this is not the case or if the signal is highly correlated, it can happen that certain paths are estimated with inaccurate contributions.

The aim of this thesis is to investigate on a simple object if the transfer paths, obtained by an Operational Transfer Path Analysis with correlated signals can be improved by additional artificial excitation on the object, for example with an impulse hammer. For this, a simple model is built with known transfer paths for airborne and structure-borne sound.

The contribution of each path is measured separately to receive a set of measurements to validate the syntheses. These syntheses are performed with the same settings on different sets of transmissibilities. Each set of transmissibilities is calculated with a CTC with constant settings, but changing excitation. The excitation leads from pure operational data to pure impulse hammer impacts and various steps in between. It will be investigated if an additional artificial excitation can help to compute the measured contributions of each transfer path.

2 Theory

In this chapter, the underlying theory of both Transfer Path Analysis (TPA) and Operational Transfer Path Analysis (OTPA) will be explained. Furthermore, a literature study about investigations on TPA methods from the last years is presented. As the measurements are performed on a small scale model, also the theory of scaled models in acoustics is briefly explained. The model might be suitable for scaled measurements, but it is not used as such for this thesis.

2.1 Literature Study

The OTPA is also known under different names, depending on the developing company. Most common are Binaural Transfer Path Analysis (BTPA) by Head Acoustics [1], Operational Path Analysis (OPA) by LMS International [2] and Operational Transfer Path Analysis (OTPA) by Müller BBM [3]. Even if they use different mathematical models and assumptions, all tools show similarities in their purpose and results. In the following literature study, all tools are commonly named as OTPA if the considered characteristic is not a unique feature of one specific product.

A good overview about the history of different TPA Methods can be seen in [3]. This paper divides the purpose of a Path Analysis into three main fields: Secrecy, Safety and Comfort. Nowadays, the main usage of TPA is the reduction of noise in vehicles and can be such seen as a comfort problem. But the trigger for the first TPA studies in the 1950s can be seen in secrecy, or more precisely the stealth of ships. With the progress of aviation and astronautics, the safety began to gain impact on the research and usage of TPA in the 1960s as increasing vibrational levels threatened the structural integrity of aircrafts and space ships. But these first steps were almost purely analytical.

The first experimental approaches were done in the early 1980s by Verheij with what is nowadays called the classical TPA, based on impulse hammer measurements [4].

The transmissibility-based TPA, that lead into the OTPA was also developed at the same time by Magrans [5], but could only be developed to a working procedure by Noumura and Yoshida around 2006 [6].

The idea of blocked forces TPA, which is a method from roughly 2000, was at first imagined in 1987 by Mondot and Petersson [7]. This method reduces the dynamics of the receiving structure to a coupling function and uses the characteristic power of a source to describe the vibration transfer. As each part is examined separately, this method is called component-based TPA.

In 2013, Roozen and Leclère showed, that artificial excitation can be used together with OTPA to figure out the number of transmission paths [8]. For that experiment, they built a model of a gearbox and used an usual hammer without force transducer to excite the setup. By using singular value decomposition they were able to detect and describe the transmissibility matrix more correctly than by using operational data with even shorter laboratory time. However, this method can't predict the influence of coherent excitation.

2.2 Transfer Path Analysis

One of the aims of the TPA is to obtain the operating forces of an exciting structure. Usually these forces are difficult to be measured directly as the usage of for example ring sensors would need too many changes in the structure to receive a reasonable result. A usual detour is to measure the transfer functions from the mounting points without the exciting structure to the receiver. With knowledge of this information, the force of the exciting structure can be calculated based on the sound measured with the operating system and the measured transfer functions. To do so, the level at the answer point is multiplied by the inverse of the transfer functions. If the transfer function is obtained by impulse hammer hits, this multiplication leads directly to the force of the real source at the excitation point.

If the system would be excited with an impulse hammer with the exciting structure attached to the receiver, a part of the induced force would go into the source component. For the determination of the operational forces by means of a matrix inversion and of the transfer function $H = \frac{p}{F}$, the sound source has therefore to be removed.

The transfer function H in $\frac{Pa}{N}$ from each interface between sound source and receiver can then be calculated, as the measured sound pressure p in Pa has only one singular source, the force of the hammer F in N.

$$H_i = \frac{p_i}{F_i} \tag{2.1}$$

If the sound source is at a position where the geometry doesn't allow it to use an impulse hammer or a shaker, it is also possible to use a reciprocal approach. This means that the excitation is not located at the source but with a volume sound source at the receiving point. With the measured acceleration at the original source, the same information can be gathered. The ratio of the acceleration a in $\frac{m}{s^2}$ at the reference point and the volume velocity q in $\frac{m^3}{s^2}$ at the answer point gives the transfer function H in $\frac{\frac{m}{s^2}}{\frac{m^3}{s^2}} = \frac{Pa}{N}$.

$$H_i = \frac{a_i}{q_i} \tag{2.2}$$

This way to obtain the transfer functions is just briefly shown here to show that many various approaches have already been made to gather the data necessary to measure the operating forces.

Other possibilities like measuring the bearing stiffness with accelerometers before and after the bearing are mostly unpracticable or have too many limitations and are therefore not further explained.

The operational forces can be determined using several techniques. In this study, the matrix inversion method is used. The usual measurement procedure is to separate the active and the passive parts and to mount indicators on the passive parts. The passive parts are then excited by the impulse hammer directly on the connection points. With this procedure, the induced force and the sound pressure or velocity at the answer points is known as well as the velocity at each indicator. By inverting this matrix and multiplying it with the sound pressure or velocity at the answer point with the real source, the operational forces can be determined.

A matrix can be inverted if at least as many indication signals as force transmissions are available. The more indication signals are measured, the more stable the matrix inversion can be calculated. If every excitation f_i leads to a different response signal a_i at the indicators, the matrix can be inverted. The inertance matrix $H_{a/f}$ can such be inverted to receive the dynamic mass matrix $H_{f/a}$.

$$H_{a/f}^{-1} = \begin{bmatrix} \frac{a_1(\omega)}{f_1(\omega)} & \frac{a_1(\omega)}{f_2(\omega)} & \cdots & \frac{a_1(\omega)}{f_n(\omega)} \\ \frac{a_2(\omega)}{f_1(\omega)} & \frac{a_2(\omega)}{f_2(\omega)} & \cdots & \frac{a_2(\omega)}{f_n(\omega)} \\ \vdots & & \ddots & \vdots \\ \frac{a_m(\omega)}{f_1(\omega)} & \frac{a_m(\omega)}{f_2(\omega)} & \cdots & \frac{a_m(\omega)}{f_n(\omega)} \end{bmatrix}^{-1} \tag{2.3}$$

In the end, the operational forces g_j can be calculated by applying the inverted matrix $H_{f/a}$ to the measured signal with the original sound source and the indicators around the mounting positions a_j.

$$\boxed{a_j \sim g_j} \xrightarrow{H_{a/f}^{-1}} \boxed{f_i} \xrightarrow{H_{p/f}} \boxed{p_i} \xrightarrow{\Sigma p_i} \boxed{P}$$

Figure 2.1: Signal processing scheme of the Transfer Path Analysis.

Even if the TPA is mostly used for investigations of structure-borne sound, it is also possible to use a volume flow source instead of an impulse hammer and microphones instead of accelerometers as indicators to get an insight on airborne sound problems.

2.3 Operational Transfer Path Analysis

The aim of the OTPA is to avoid taking the structure of interest apart and to use only operational measurements. This is done by defining reference planes, where sensors are located to measure the acceleration or the sound pressure at this point.

If the operational forces are not of interest but only the transfer path contributions, it is also possible to use a method developed from the TPA, the Operational Transfer Path Analysis. The big advantage of this method is that it's not necessary to remove the sound source. Additionally, no forces or pressure flows have to be measured. The analysis is based on so called reference signals, like velocities and sound pressures close to the source.

$$\boxed{a_j} \xrightarrow{H^{-1}_{a/p}} \boxed{p_j} \xrightarrow{\Sigma p_j} \boxed{P}$$

Figure 2.2: Signal processing scheme of the Operational Transfer Path Analysis.

In a linear system, the response signal Y can always be directly calculated from the input signal X with the transmissibility H. While the traditional TPA method explained above only has one single excitation per measurement, the OTPA has to detect the different paths from measurements with multiple sound sources. A requirement for the Operational Transfer Path Analysis (OTPA) is the appropriate location of the indicator sensors and a variety of excitation signals. This way, the excitation of the receiver during operation can be described simultaneously at various points. The differentiation of the paths is done by crosstalk cancellation (CTC), based on the statistical methods singular value decomposition (SVD) and Principle Component Analysis (PCA) [9]. The CTC extracts the transmissibilities $\frac{H}{a}$ from the operational data. These are later used in a transfer path synthesis to determine the contribution of each reference to the answer point.

To receive a correct reproduction of all transfer paths it is important to set the reference planes of the object of interest correctly. A reference plane should be a plane in the object in which the transfer paths of interest can be clearly separated from all others. If one transfer path can be described on multiple measurement points on the reference plane it should be considered to change the plane. It might not be explicitly possible to describe the path correctly with this set of measurement points.

The OTPA is usually combined with a TPS, a synthesis of the level at different places on the reference planes with the aim to investigate the level of each measured path. By combining different paths, the contribution by for example structure-borne sound or two paths joining at a point closer to the answer can be calculated.

2.4 Physical models in Acoustics

Physical models are a widely used tool in various fields of acoustics. Measurements on scaled physical models can be traced back to the 1930s in room acoustics [10], but since then also in building acoustics [11], environmental acoustics [12] and automotive acoustics [13], different physical models were used to investigate particular qualities with reasonable effort.

For measurements using scaled models considering only airborne sound, the frequencies have to be adjusted to the dimensions of the structure. So if a room is supposed to be rebuilt in the scale 1:10, the frequency range also shifts up by a factor 10. For room acoustical and environmental acoustical scaled measurements, only few properties like air attenuation and the absorption factors of the materials have to be adjusted as well. For geometrical investigations the models usually show a good agreement to a not scaled object.

For structure borne sound, the scaling becomes more difficult, as the speed of sound might be frequency dependent and it might be difficult to find materials with a matching shift in the dispersive aspects.

3

Model

In this chapter, the setup built to perform the measurements is described and explained. The setup consists of two chambers: the left one can be seen as source structure or sending box, the other one is the receiver structure or receiving box. These two are connected by three connecting bars for structure-borne sound and one channel for airborne sound. Each path can be removed and therefore be examined individually.

In the sending box two exciters are located in one corner on a metal mount to excite structure-borne sound. In the adjacent corner, one loudspeaker is placed for airborne noise.

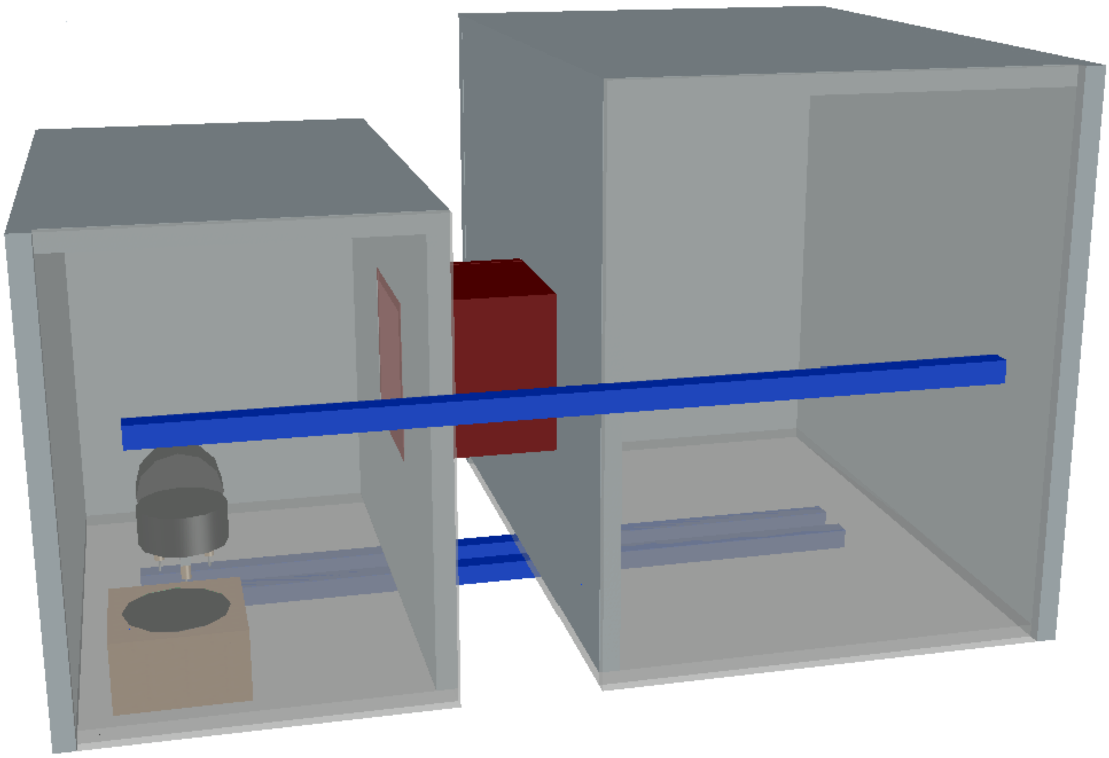

Figure 3.1: Drawing of the measurement model. The bars (blue) are used to transmit structure-borne sound while the channel (red) is the airborne sound connection.

3.1 Measurement Environment

To obtain a closed measurement environment, a model was built to have known airborne and structure borne sound propagation. The structure borne sound is excited by two exciters on a steel mount that is further described in subsection 3.2.1. All coupling elements between excitation points and the measurement points are made in either acrylic glass or any kind of metal, resulting in homogenous materials with known properties. Three metal bars connect the two chambers. The bar on the side, later called bar 3, is attached to the acrylic plates by four screws, two on each plate. The two bars on the floor have in addition to those screws also two (bar 1, further back) or one (bar 2) screws where the exciter mount is firmly connected to both the acrylic glass and the bar. Each bar has the same length of 78.5 cm and is made of a quadratic aluminium pipe with an inner side length of 1.6 cm and a wall thickness of 0.2 mm.

The airborne sound cavities are made from coated chipboard and acrylic glass. The structure-borne sound propagation occurs only on the glass plates, the purpose of the wooden plates is to shield the setup from exterior noise and to have a known environment. The acrylic glass has a thickness of 12 mm. This was decided as it is sufficiently stable while also having an adequately high coincidence frequency. The wavelength in air is calculated in accordance to Equation 3.1 and the equation for the wavelength of bending waves in acrylic glass is shown in Equation 3.2. λ is hereby the wavelength, c_{air} is the speed of sound in air with the value of 343 $\frac{m}{s}$ and f is the frequency. For the speed of sound of bending waves, also the Young's modulus E, the thickness of the material d, the density ρ and the loss factor μ are needed for calculation [15]

$$\lambda_{\text{air}} = \frac{c_{\text{air}}}{f} \tag{3.1}$$

$$\lambda_{\text{B}} = \sqrt[4]{\frac{\frac{E \cdot d^2}{12(1-\mu^2)}}{\rho}} \cdot \sqrt{\frac{2\pi}{f}} \tag{3.2}$$

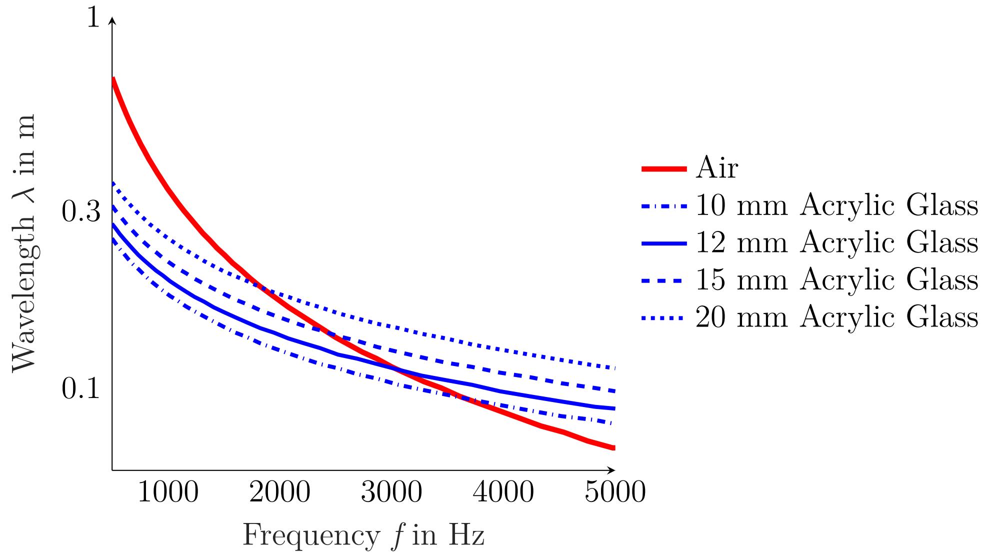

Figure 3.2: Wavelength in air and of bending waves in acrylic glass

The sound propagation to the receiving box happens through a wooden channel with an inner side length of 11 cm. The channel is 16.5 cm long and attached to both boxes with a press fit. It can be closed with wooden plates and filled with mineral wool to suppress airborne sound propagation.

The whole construction is supported by elastic layers. The stiffness of the layers and the weight of the model is tuned to have its resonance frequency around 50 Hz.

The coupling of the structure-borne sound between the sending and the receiving box was decided to be made by three aluminium bars. These are mounted directly underneath the exciting structure as well as on the adjacent acrylic plates. Each bar is mounted with four screws on the acrylic plates. The exciting structure is mounted with three screws on both the acrylic glass and the aluminium bars.

3.2 Exctitation

To excite the setup with known signals, one loudspeaker and two bending wave exciters were used. Those commercial parts were tried to be assembled on a small structure to achieve an excitation similar to an engine in a car, where torque, vibration and airborne sound emerges at roughly the same place. Two mounting brackets, a plate based structure and beam based smaller structure, were built and examined to obtain an optimal excitation of the whole system. For the airborne sound excitation, a 10.2 cm broad band loudspeaker was built into a wooden box.

3.2.1 Structure-borne sound

3.2.1.1 Plate based mount

A first mounting structure was built from steel plates with similar dimensions as the exciters. This was decided as the exciters are supposed to be mounted on a plate to stimulate bending waves.

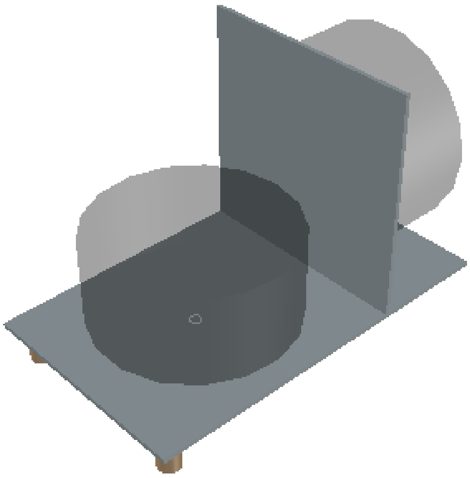

Figure 3.3: Drawing of the plate structure.

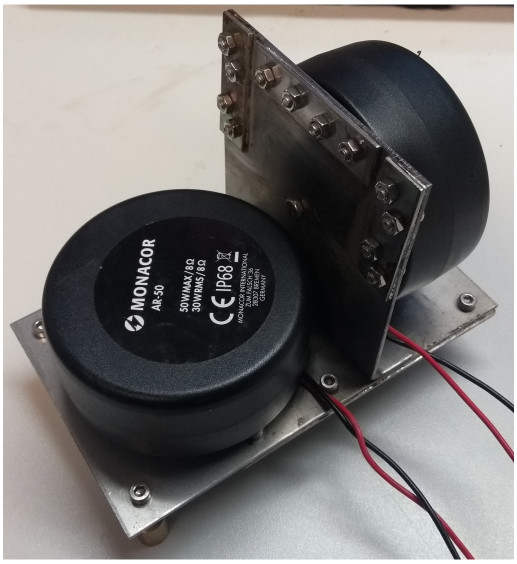

Figure 3.4: Picture of the plate structure with soldered and screwed bars with attached exciters.

3.2.1.2 Bar based mount

As the plate based mount was too soft and vibrated too much it was decided to build a stiffer holder for the exciters. A welded structure made from steel bars seemed like a possibility to achieve good results with reasonable effort.

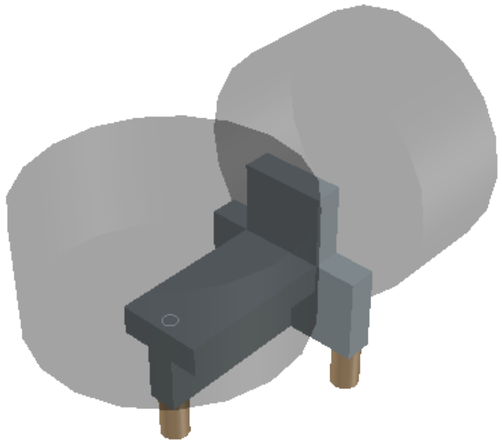

Figure 3.5: A very stiff mount option with bearings and outlined exciters, consisting of four welded bars.

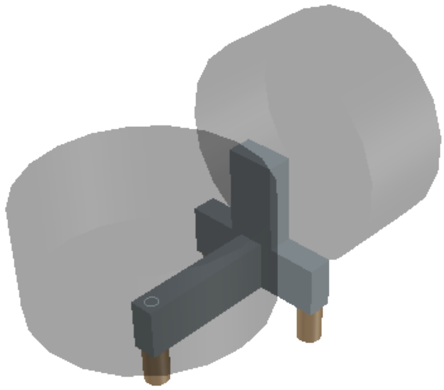

Figure 3.6: A simplified mount option with bearings and outlined exciters, consisting of three welded bars.

To attach the mount on the acrylic glass, different column bearings can be used. All bearings have the same height of 15 mm and the same M04 threads on both sides. One set of bearings is made of brass with a diameter of 10 mm to obtain a rigid connection. The other two are rubber buffers with 10 mm and 15 mm diameter. The different bearings were intended to investigate the structure borne sound transmission change between the mount and the acrylic glass but weren't used in the end.

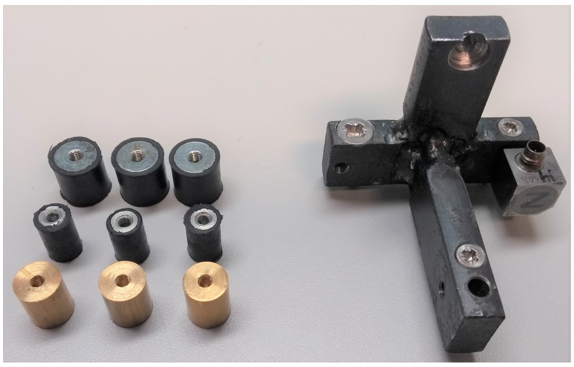

Figure 3.7: Picture of the bar based structure and the different footings. Attached to the structure is a three-dimensional accelerometer.

3.2.2 Airborne sound

The 12 mm acrylic plates are framed by 19 mm coated chipboard plates, resulting in an enclosure with known airborne sound properties. The dimensions of the resulting boxes were chosen such that in the frequency region where most measurements were supposed to happen, a sufficient high modal density could be reached. The sending box has an inner height of 40 cm, a length of 50 cm and is 30 cm broad. The receiving box is 10 cm larger in each dimension. The frequencies of the modes, calculated in accordance to Equation 3.3 [14], are shown in Figure 5.4.

$$f = \frac{c_0}{2}\sqrt{\left(\frac{N_x}{L_x}\right)^2 + \left(\frac{N_y}{L_y}\right)^2 + \left(\frac{N_z}{L_z}\right)^2} \tag{3.3}$$

3.3 Physical modifications

To verify the assumptions made in the measurement setup, various measurements were performed. This was also necessary to check if the results of the OTPA are reliable.
The measurements were performed on July 11 2019, in the afternoon, in the anechoic chamber at the Müller-BBM Headquarter in Planegg close to Munich, Germany. During the measurement period, the temperature in the room was stable between 25.5 °C and 25.8 °C and the humidity rate remained between 39 % and 43 %.

3.3.1 Signals

The measurements were performed to check the sound contribution of each source and the influence of each transfer path. For this measurement, all sources were excited with white noise, bandpass-filtered from 200 Hz to 5 kHz. The frequency range was chosen as lower frequencies are usually dominated by modes. In higher frequencies, the wavelength is in the same range as the size of the sensors and therefore no phase information can be gained reliably.

In most applications the airborne sound contribution is significantly lower than the structure-borne part. Therefore, the volume was scaled so the unweighted total sound pressure level in the receiver box from the two exciters was about 10 dB higher to the one produced by the loudspeaker if all paths were available.

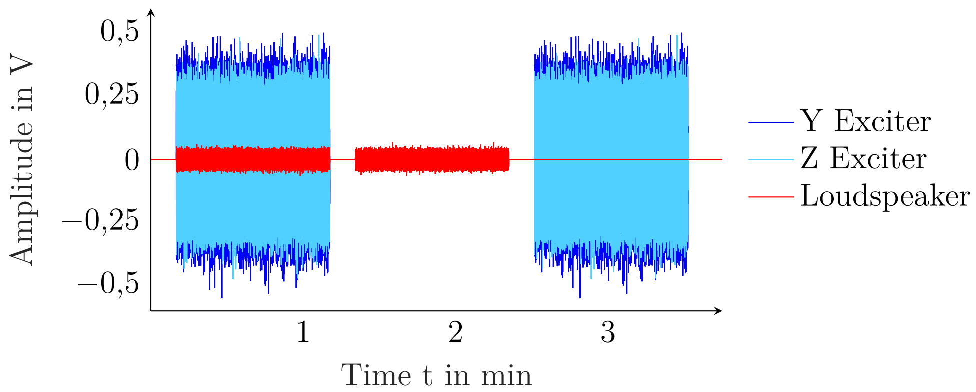

Figure 3.8: Output signal for all measurements. In the following, the first minute with all sources is signal 1, the second minute with only the loudspeaker active is signal 2 and the minute with both exciters is signal 3.

With these signals, the airborne and structure-borne sounds were excited both separately and combined. The signal used for the combined and separate excitation was the same and was generated just once for all measurements.

3.3.2 Setups

To measure the influence of each transfer path on the sound pressure level in the receiving box, each connection was measured separately. With this measurements, the results of the TPS can be verified, as the contribution of each path found by the OTPA has to fit these measurements.

Setup	Bar 1 & 2	Bar 3	Channel for airborne sound
1	attached	attached	open
2	removed	removed	open
3	removed	removed	closed
4	removed	attached	closed
5	attached	removed	closed
6	attached	attached	closed

Table 3.1: Setups used to investigate the influence of each transfer path.

The combinations with only one structure-borne sound connection attached and the airborne sound channel open were not measured as no investigation on these combinations were planned.

All measurements were performed twice. Each screw was always attached at the same position with a torque wrench set to 2 Nm. During the measurements, the anechoic chamber was empty except for the necessary cables and the measurement setup. The ventilation system was shut down and the lights were switched off. The sending box had to be left open for the measurements, as excitation with an impulse hammer was not possible otherwise.

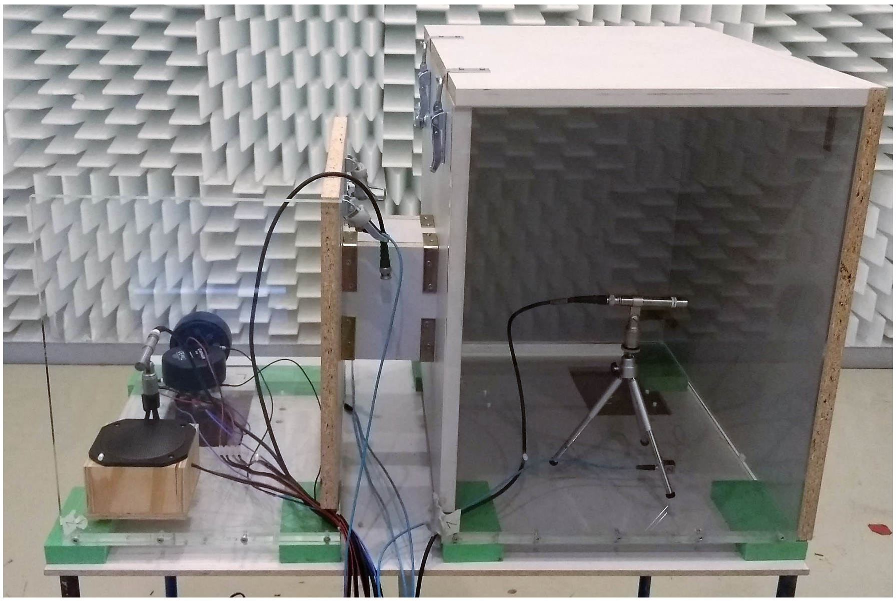

Figure 3.9: Setup 3, with removed bars and closed airborne sound channel.

4

Measurements

All following measurements were performed with the whole system, Setup 1 from section 3.3. The measurements were performed in the same room and on the same day as the previous ones.

4.1 Equipment and Calibration

All microphones and accelerometers have been calibrated before and after the measurements were performed on July 11 2019. The location, position, direction and the calibration difference of each sensor before and after the measurements are shown in Table A.2. The position is also shown in Figure 4.1. Detailed information about the measurement equipment can be seen in Table A.3.

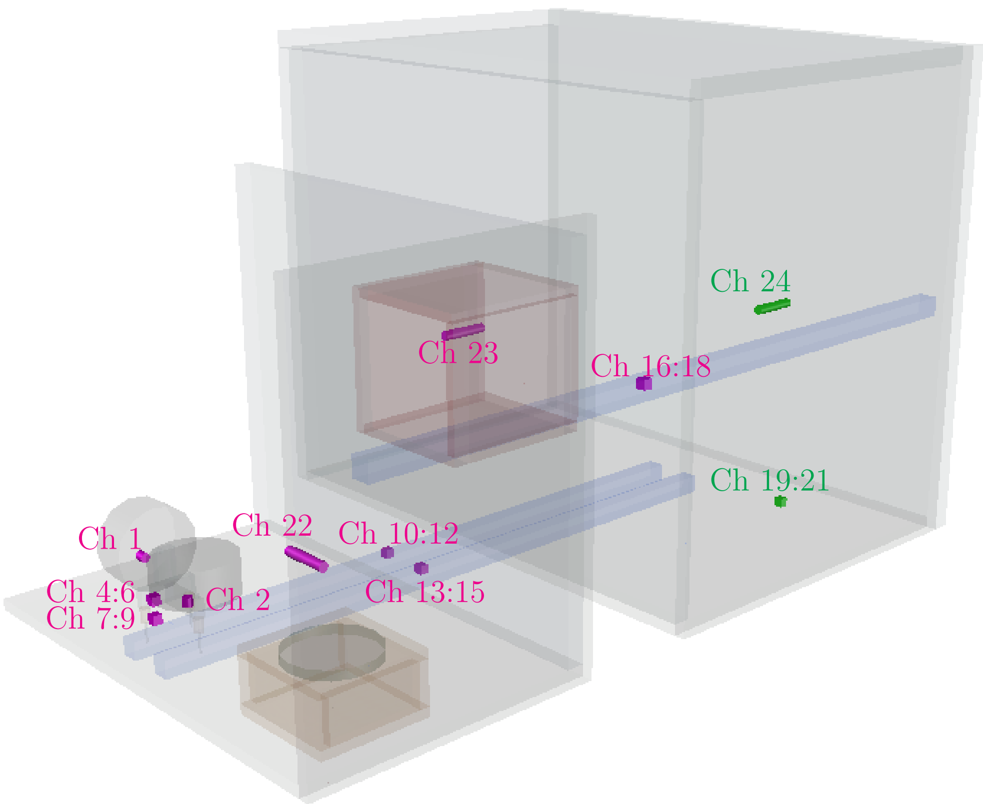

Figure 4.1: Accelerometer and microphone positions. All reference sensors are marked magenta, the answer sensors are shown in green.

Figure 4.1 shows the location of each sensor. Some of the sensors, for example the green one in the receiving box, are triaxial accelerometers. These are mounted at one point but measure the acceleration in all three spatial dimensions. Therefore, the location of three channels in Table A.2 is identical, but the direction varies. As the output of the sensor is fixed, the direction of each channel had to be set in accordance to the location of the cable and is not always +X for the first channel of the sensor, +Y for the second one and +Z for the third channel.

For the OTPA measurements, a cable was connected directly from the loudspeaker amplifier to the MKII measurement system. For the impulse hammer measurements, the hammer was connected to the same input channel.

For all measurements, the sampling frequency was 22050 Hz. The FFT was performed for the whole signal length of 60 s with a blocksize of 8192 samples without overlap.

4.2 Impulse Hammer

To see if the OTPA can be improved by additional artificial excitation, measurements on various points using an impulse hammer were performed. The 16 measurement positions stated in Table A.1 are partitioned into three groups:

- H1 The first six positions are located before the source, so on the housing of the exciters. These locations can be assimilated to hitting with the hammer anywhere on the motor in a car if the transfer paths from the motor to the driver are to be investigated.
- H2 The second four positions are on the metal mount, so after the source but still before the interface. The analogy to this would be hitting the screws of the engine suspension with an impulse hammer.
- H3 The third group of hammer positions is placed on the connection bars. From this, it can be deduced if artificial excitation anywhere on each transfer path could help improving the result.

4.3 OTPA

4.3.1 Reference planes

For the Operational Transfer Path Analysis the excitation signals shown in subsection 3.3.1 were used. The reference planes are shown in Table 4.1 and Figure 4.2.

Name	Location	References
i	On the sources	1-3
ii	On the mount	4-6, 22
iiC	On the mount	4-6, 23
iii	On the acrylic glass	7-9, 22
iv	Connections between the boxes	10-18, 23

Table 4.1: Reference planes for the OTPA.

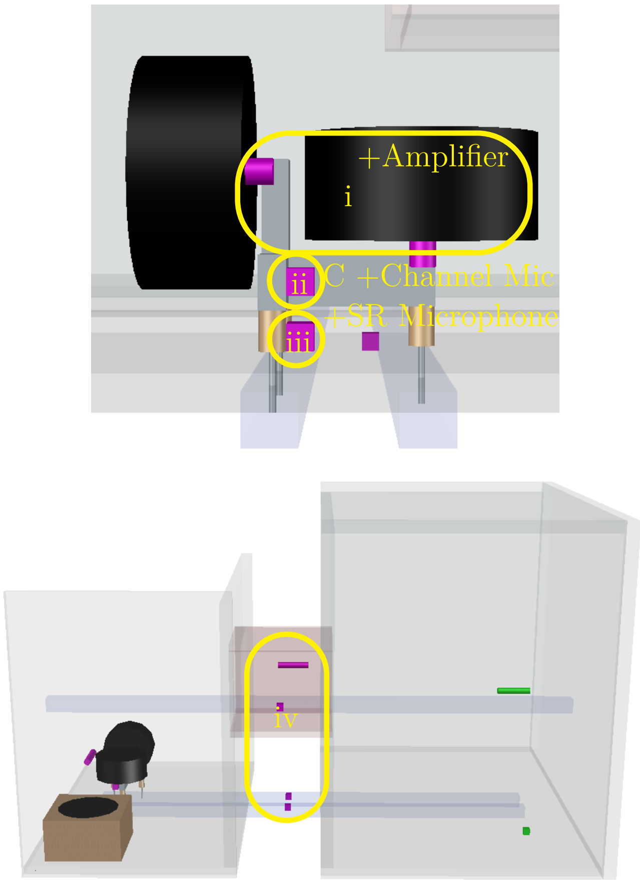

Figure 4.2: Reference planes for the OTPA.

Reference plane i contains the structure-borne excitation directly from the exciters and the amplifier output. Therefore it has to be able to differentiate the airborne and structure-borne sound contributions correctly, if the OTPA works properly.

The planes ii and iii should reveal very similar results, as they are located very close to each other. Both should be able to calculate at least the structure-borne sound content correctly. The airborne sound is with this setup always a mixture between the noise produced by the loudspeaker and secondary airborne sound from the exciters. Plane iiC has the same structure-borne sound information as ii, but it uses the microphone in the channel to calculate the airborne sound contribution.

In a perfect OTPA, plane iv should show exactly the same results as the investigation with physical modifications shown in subsection 5.2.2. It is the only reference plane that can differentiate between the bars.

4.3.2 Crosstalk cancellation

The CTC of an OTPA can be performed using various parameters that can influence the result quite substantially. The CTC for this thesis was performed using a normalisation, meaning that the levels of all input channels were normalised. If this option is disabled, a sound pressure will have a much higher influence on each path than an acceleration, as the value is much larger.

The second setting made identical for all CTCs was the method to separate the paths. This option was set to 95 % cumulative contribution. This means, that 95 % of the detected principal components were used to perform the CTC. The last few principal components usually contain only noise produced anywhere in the measurement chain. If less than 95 % of all principal components were used, the complex transfer function between all references and the answer points was stable. Therefore, this value was used to perform all CTCs as it can be assumed that all the noise was in the 5 % that have been skipped.

The references used to calculate the CTCs are shown in Table 4.1. The answer position for all calculations was always channel 24, the microphone in the receiving box.

4.3.3 Synthesis networks

Synthesis networks are a visualisation of calculations performed in the Transfer Path Synthesis. In the used software from Müller-BBM called PAK, the most important calculations are sources, transmissibility matrices and additions. A synthesis network has to be set for each reference plane. The result of the synthesis can be obtained at different points in the network, and therefore these results can be verified with the physical modifications.

An input to a calculation is always marked with a red box while an output can be shown in green or blue. A blue output will be saved while both green and blue outputs can be connected to an input. Each out- and input has to be specified with one channel. Every input needs to be connected to an output, which is marked in the software with a blue line. The networks shown in the following are such a graphical representation of the calculations made by the software.

A source provides measurement data that are fed into a transmissibility matrix, where the designated answer and the reference have to be set to the same positions as in the source, to receive parallel connections. After the transmissibility matrix, multiple outputs can be added into a combination.

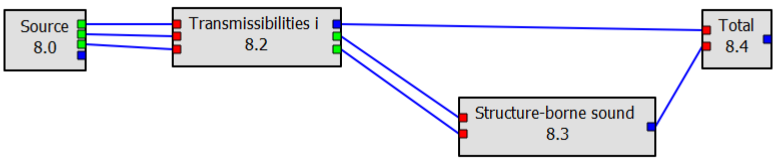

Figure 4.3: Synthesis network for reference plane i.

In this network, the source contains the channels 3, 1, 2 and 24 of a measurement with both sources active. This means that the first output is the voltage of the amplifier, the second and third are the sensors on the exciters Y and Z and the last output is the sound pressure in the receiving box. The last one is saved directly and only used for further comparison.

The other three channels are fed into the transmissibility matrix, where they are multiplied with the transmissibilities from their position to the receiving box microphone calculated in the CTC. The airborne sound contribution is saved and also fed into the addition for the total sound pressure synthesis in the receiving box. The two structure-borne sound paths are added to a structure-borne sound contribution which is as well saved as fed into the total sound pressure synthesis in the receiving box.

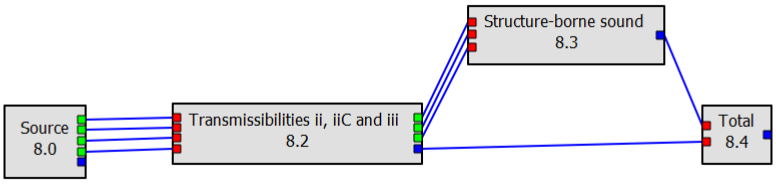

Figure 4.4: Synthesis network for reference plane ii, iiC and iii.

This network is similar to the one for plane i. The structure-borne sources at the mount or on the acrylic glass go from the source to the transmissibility matrix and are added to a structure-borne sound contribution before being added to the airborne sound contribution to receive a sound pressure synthesis in the receiving box.

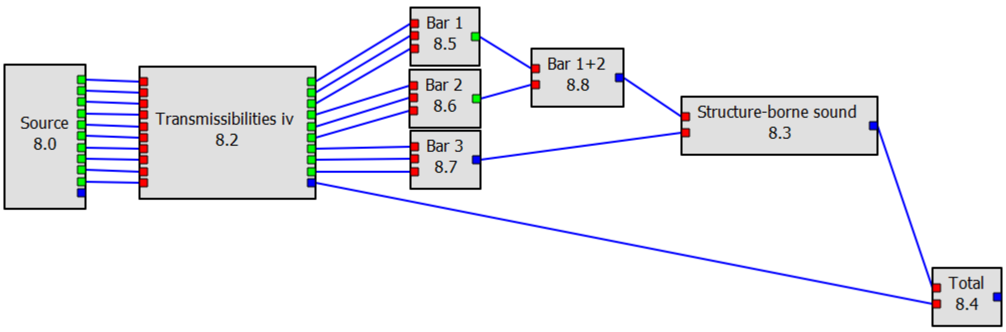

Figure 4.5: Synthesis network for reference plane iv.

The network shown in Figure 4.5 is the most complex one used in this thesis. The transmissibilities in all three directions on each bar are first added separately, then the two bars on the floor are added, saved and passed on to the total structure-borne sound contribution together with bar 3. The airborne sound contribution is calculated from only one microphone, therefore no further calculation is needed except for the addition with the structure-borne sound to synthesize a sound pressure in the receiving box.

5

Results

5.1 Model

5.1.1 Excitation

The plate structure was found to have strong eigenfrequencies in the frequency region of interest from 500 Hz to 2 kHz. At those eigenfrequencies, the plates started to vibrate strongly, which resulted in audible peaks and noise. A stiffening of the structure with screwed and soldered metal bars only changed the frequency of the eigenmodes slightly but didn't solve the problem.

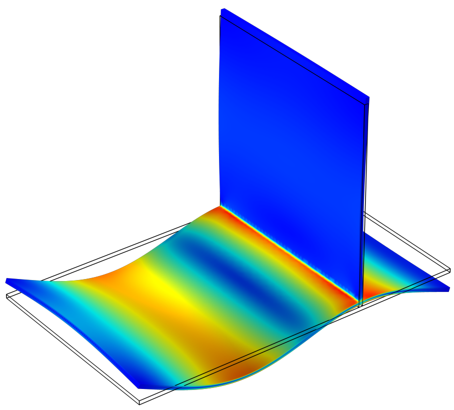

Figure 5.1: An Eigenmode of the plate structure at 851.7 Hz. This mode corresponds with a measured mode at 830 Hz of the plate structure without stiffening steps.

The measured frequencies of those modes corresponded well with FEM simulations performed in Comsol, so it was decided to first simulate other structures before they were built.
Different possibilities were simulated with a FEM program and the resonance frequencies were calculated. The highest eigenmodes could be detected in structures with a T-like support for the horizontal exciter as shown in Figure 3.6. As it was planned to only consider frequencies up to 2000 Hz, the simplified version with only an I-like support was simulated, found suitable and was therefore built.

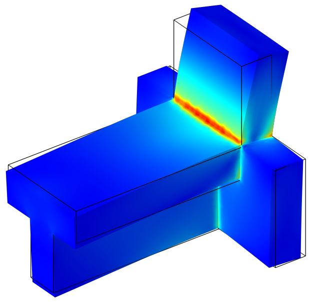

Figure 5.2: First Eigenmode of a possible mount at 8506.4 Hz.

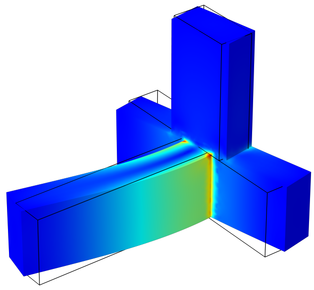

Figure 5.3: First Eigenmode of the built mount at 4692.8 Hz.

5.1.2 Box modes

The box modes were calculated in accordance to Equation 3.3 for both boxes.

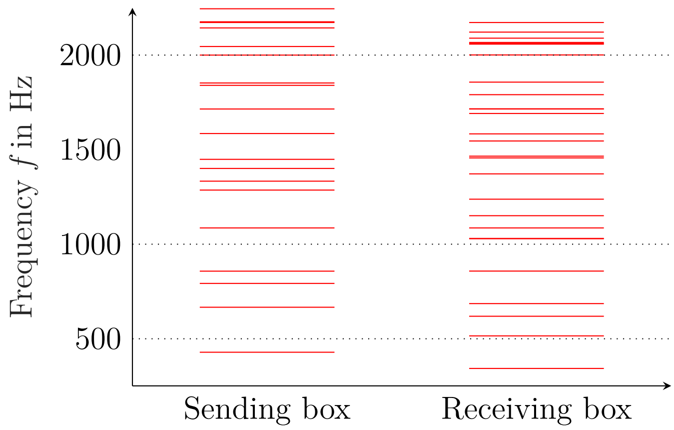

Figure 5.4: Modes in the boxes

To see the influence of the removed walls of the sending box, another measurement was performed with setup 1 from section 3.3 and a closed sending box. In this measurement, all 1/3 octave band levels were about 10 dB higher but showed the same development regarding the switched-on sources. If the small band spectrum is reviewed, some of the box modes can be observed as it can be seen in Figure 5.5.

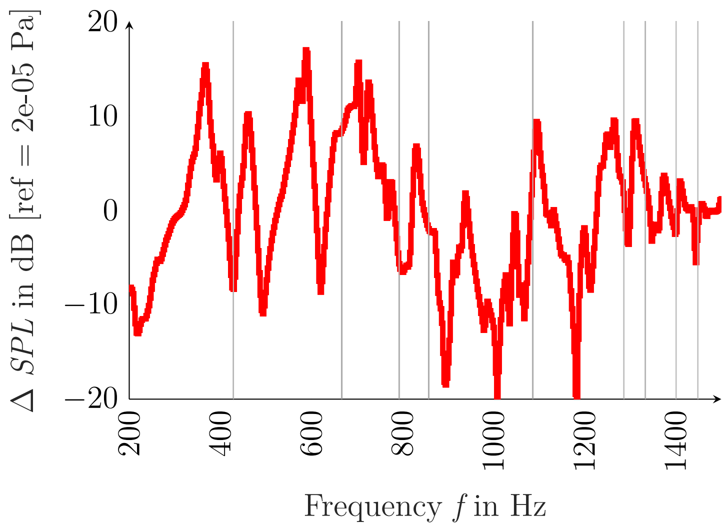

Figure 5.5: Difference between the sound pressure level in the sending box with and without closed box in red and calculated frequencies of the box modes as vertical lines in grey.

For Figure 5.5, the sound pressure level with open box was subtracted from the SPL with closed box. This way, a lower level with the closed box leads to a negative value.

5.2 Physical modifications

5.2.1 Reproducibility of the measurements

To see if the setup was reproducible, all measurements were performed twice. This was done in a way that first all measurements were performed from Setup 1 to 6 and then backwards from 6 to 1.

The sound pressure level (Figure 5.6) and the acceleration level in Z-direction (Figure 5.7) in the receiving box were chosen to show the reproducibility. In this section, the left figure shows the first measurement, on the right side the second run is shown.

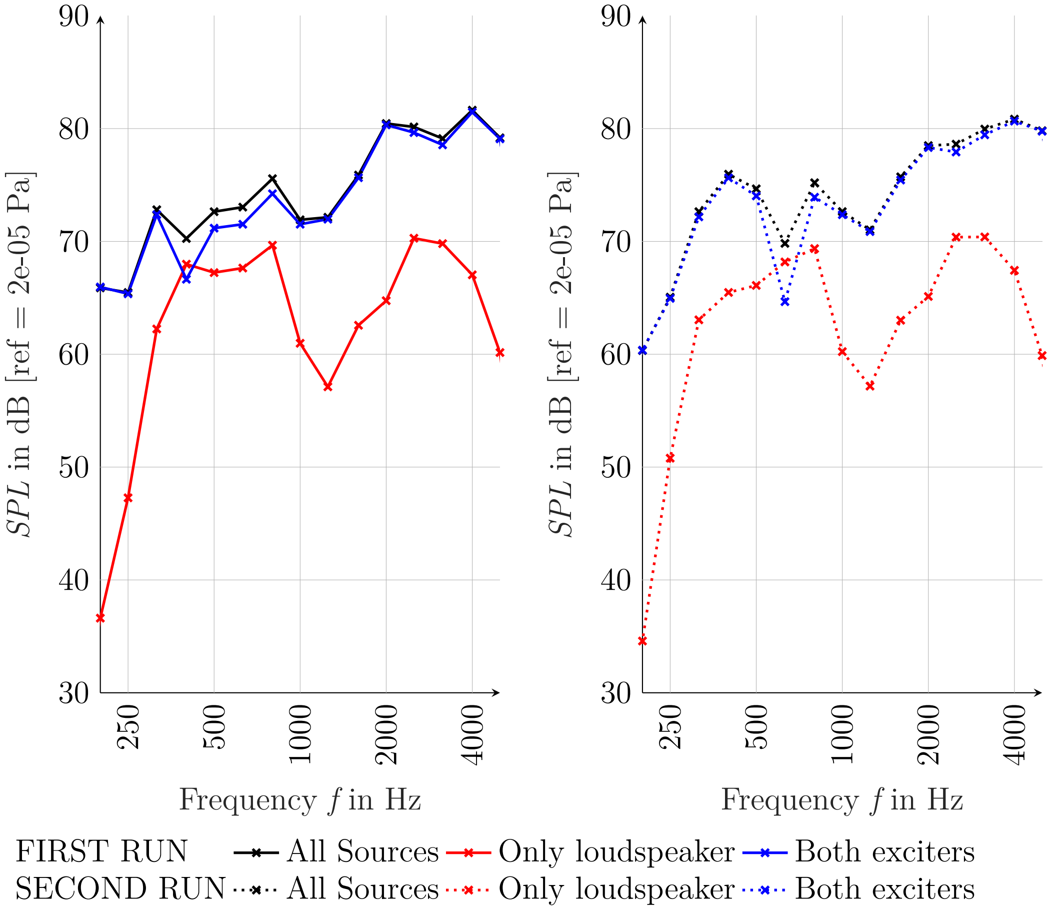

Figure 5.6: Sound pressure level in the receiving box in setup 1.

The sound pressure level in the receiving box is dominated by the sound produced by the exciters, but the two measurement runs lead to a good match of the results above 1000 Hz.

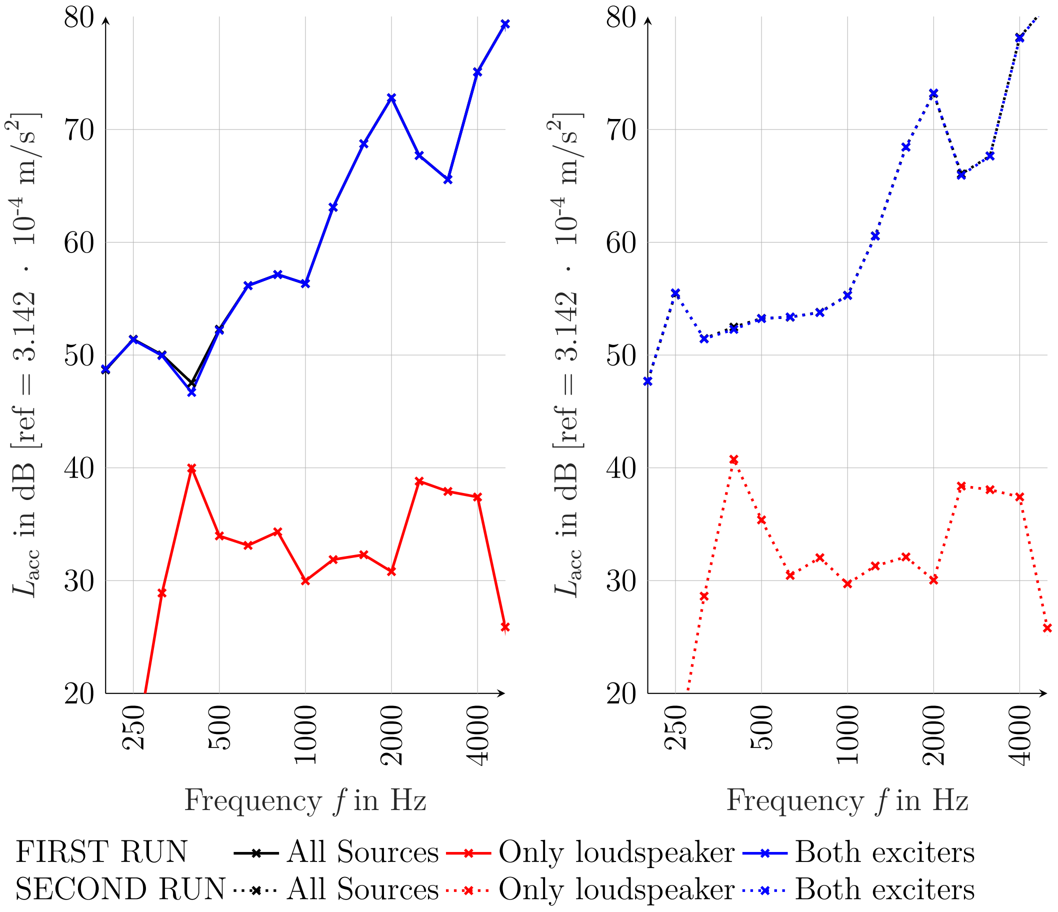

Figure 5.7: Acceleration level in the receiving box in setup 1.

When the acceleration in the receiving box is reviewed, the domination of the sound produced by the exciters is even higher.

5.2.2 Estimation of the influence of each transfer path

The sound pressure level measured in the receiving box with each setup from the first measurement run is shown in 1/3 octave bands in Figure B.1 and as a single value in Table 5.1.

Table 5.1 shows the setups explained in Table 3.1 briefly on the left side with + meaning attached, - removed, o open and c closed. The left side shows the unweighted total sound pressure level in the receiving box.

	Setup			Sources		
	B1 & 2	B3	Channel	All Sources	Loudspeaker	Exciters
1	+	+	o	87.7	75.2	87.5
2	-	-	o	83.6	75.1	82.9
3	-	-	c	68.5	52.0	68.5
4	-	+	c	81.8	52.5	81.8
5	+	-	c	84.6	51.9	84.6
6	+	+	c	85.2	52.7	85.1

Table 5.1: Unweighted total sound pressure level in the receiving box from 1000 Hz to 5000 Hz in dB [ref = 2 E-5 Pa] of each setup and source combination from Figure B.1

5.3 Measurements

5.3.1 CTC using operational measurements - Shift of reference planes

To investigate if the OTPA works correctly and where something could be improved by using additional artificial excitation, a CTC was performed using only the operational measurements. Therefore, the reference planes shown in subsection 4.3.1 were used.

An OTPA gives an almost perfect result if the same signal is used for the CTC and the TPS as it does the same calculation twice in opposite directions. Therefore, the CTC in all following calculations was performed using the measurements with alternating sources, signal 2 and 3, and the input for the TPS was the combined measurement, signal 1.

In the following, the results of the transfer path syntheses are shown in a table as single values together with the measured sound pressure levels of the appropriate setup from subsection 5.2.2. The single values are the unweighted sound pressure levels, summed from 1 kHz to 5 kHz, as this frequency range was found to be well reproducible.

Measurement T means that all sources were active to obtain these results, meaning that different values result from the different setups. For measurement S, the sources planned to radiate the matching kind of sound were used, so for the contribution from air only the loudspeaker was used and for the other contributions only the exciters were active. The Total is of course the same as all sources had to be active.

Only the reference plane iv had sensors on each bar and is therefore able to detect the influence of these paths separately.

		Total	Air	Contribution from Structure	B1 & 2	B3
Measurement T	Setup	1	2	6	4	5
	Signal	1	1	1	1	1
Measurement S	Setup	1	2	6	4	5
	Signal	1	2	3	3	3

Table 5.2: Explanation of the difference between the Measurements T and S used in Table 5.3, with the use of the setups introduced in Table 3.1 and the signals shown in Figure 3.8.

	Total	Air	Contribution from Structure	B1 & 2	B3
Measurement T	87.7	83.6	85.2	84.6	81.8
Measurement S	87.7	75.1	85.1	84.6	81.8
Plane i	87.2	74.7	86.9	-	-
Plane ii	87.1	75.8	86.8	-	-
Plane iiC	87.2	84.5	86.1	-	-
Plane iii	87.2	76.2	86.9	-	-
Plane iv	87.3	84.3	86.7	85.6	73.6

Table 5.3: Unweighted summed sound pressure level from 1000 Hz to 5000 Hz in dB [ref = 2 E-5 Pa] of the measurements and synthesis results without additional excitation on all reference planes.

5.3.2 CTC using Hammer measurements

The CTC can be performed not only using the operational data, but also with the frequency data of the hammer measurements. This data is not the usual application of a CTC, but to see the possible influence of the impulse hammer measurements it is nonetheless worth to contemplate.

The impact points are divided into three groups as it is shown in section 4.2. In the following, the hammer measurements are reviewed in each group, called H1, H2 and H3, as well as combined, which is called H123. As each hammer measurement can be combined with each reference plane, only the planes iiC and iv were considered. The input signal for the TPS was the same as the one used for the OTPA, signal 1 from Figure 3.8.

		Contribution from	
	Total	Air	Structure
Measurement	87.7	83.6	85.2
H1	91.7	91.2	81.3
H2	94.5	94.3	80.9
H3	109.8	97.0	109.5
H123	99.7	89.7	99.3

Table 5.4: Unweighted summed sound pressure level from 1000 Hz to 5000 Hz in dB [ref = 2 E-5 Pa] of the measurements and synthesis results with only hammer impacts in reference plane iiC.

			Contribution from		
	Total	Air	Structure	B1 & 2	B3
Measurement	87.7	83.6	85.2	84.6	81.8
H1	88.9	81.8	88.2	87.0	79.3
H2	89.2	86.2	87.5	86.9	78.0
H3	93.1	88.7	91.5	91.1	80.3
H123	92.3	88.3	90.7	90.2	81.0

Table 5.5: Unweighted summed sound pressure level from 1000 Hz to 5000 Hz in dB [ref = 2 E-5 Pa] of the measurements and synthesis results with only hammer impacts in reference plane iv.

5.3.3 Combination of operational and impulse hammer measurements

The goal of this thesis is to investigate the combination of operational measurements and impulse hammer measurements for OTPA. After all influences have been investigated separately, the combination is made in this section.

		Contribution from	
	Total	Air	Structure
Measurement	87.7	83.6	85.2
w/o Hammer	87.2	84.5	86.1
H1	87.0	83.7	81.3
H2	86.5	84.2	80.9
H3	90.2	89.3	109.5
H123	97.3	96.8	99.3

Table 5.6: Unweighted summed sound pressure level from 1000 Hz to 5000 Hz in dB [ref = 2 E-5 Pa] of the measurements and synthesis results with operational data and additional artificial excitation in reference plane iiC.

			Contribution from		
	Total	Air	Structure	B1 & 2	B3
Measurement	87.7	83.6	85.2	84.6	81.8
w/o Hammer	87.3	84.3	86.7	85.6	73.6
H1	87.2	83.8	86.5	85.4	74.0
H2	87.2	82.9	86.2	85.2	76.5
H3	88.3	87.0	88.4	87.8	80.8
H123	88.0	86.7	88.2	87.6	80.9

Table 5.7: Unweighted summed sound pressure level from 1000 Hz to 5000 Hz in dB [ref = 2 E-5 Pa] of the measurements and synthesis results with operational data and additional artificial excitation in reference plane iv.

5.3.3.1 Amount of impulse hammer impacts

For all previous syntheses, the CTC was performed with all impulse hammer impacts for the selected position. To derive a measurement rule for future application, the effect of the amount of impacts was also considered relevant. One impact means hereby a single impact at each location of the set.

			Contribution from		
	Total	Air	Structure	B1 & 2	B3
Measurement	87.7	83.6	85.2	84.6	81.8
w/o Hammer	87.3	84.3	86.7	85.6	73.6
1 Impact	87.3	84.8	87.2	86.7	81.2
5 Impacts	87.7	86.0	88.2	87.8	81.8
10 Impacts	87.8	86.7	88.3	87.7	80.8
20 Impacts	88.3	87.0	88.4	87.8	80.8

Table 5.8: Unweighted summed sound pressure level from 1000 Hz to 5000 Hz in dB [ref = 2 E-5 Pa] of the measurements and synthesis results with operational data and additional artificial excitation in reference plane iv with a different number of impulse hammer impacts.

5.3.3.2 Necessity of impacts on all paths

The results of this thesis have shown so far that a decent amount of impulse hammer impacts is sufficient if the reference plane was chosen correctly to improve the OTPA. It will be now investigated if every path has to be artificially excited to get this result. Therefore, the CTC and TPS were also performed with just the impacts on each connection separately, impacts in just one direction, and finally one single impact on Bar 3 from the top as this one is the easiest point to hit.

			Contribution from		
	Total	Air	Structure	B1 & 2	B3
Measurement	87.7	83.6	85.2	84.6	81.8
w/o Hammer	87.3	84.3	86.7	85.6	73.6
All Bars	87.7	86.0	88.2	87.8	81.8
Bar 1 and 2	87.7	86.8	88.6	87.7	83.5
Bar 3	87.3	84.6	87.4	87.3	79.6
All Bars z	87.5	86.6	88.6	88.4	82.1
Bar 3 z	87.3	84.0	86.5	86.1	76.3

Table 5.9: Unweighted summed sound pressure level from 1000 Hz to 5000 Hz in dB [ref = 2 E-5 Pa] of the measurements and synthesis results with operational data and additional artificial excitation in reference plane iv with 5 impulse hammer impacts on different paths of the reference plane.

6
Discussion

6.1 Physical modifications

6.1.1 Box modes

Figure 5.5 shows a good coincidence of the modes in some frequencies. The high amplitude differences around 400 Hz and 1100 Hz indicate the influence of room modes at some frequencies.

In the receiving box, the calculated box modes have a lower coincidence with the measured sound pressure level differences. This can be deduced from the interference of the modes in both boxes measured in one box.

6.1.2 Reproducibility of the measurements

Figure 5.6 shows a high deviation at lower frequencies. Therefore it was decided to only consider the higher range between 1 kHz and 5 kHz for further conclusions. This deviations are to be deduced to small changes in the setup, and thus a discrepancy in the transfer paths between the two boxes.

If the acceleration level is reviewed, the deviation between the measurements is higher, so it was decided to use only the sound pressure level as answer point for the OTPA.

6.1.3 Estimation of the influence of each transfer path

Comparing the setups 1 and 2 in Table 5.1, the bars have basically no influence on the airborne sound propagation from the loudspeaker. A comparison between the different sources in setup 2 also shows, that the exciters produce a significant amount of airborne sound in the sending box and such in the receiving box.

The contribution of the bars is shown in the case of the closed airborne sound channel, setup 3 to 6. The bars directly below the source have a higher contribution than the one on the side. The nonetheless high level with only bar B3 attached can be derived to the good sound propagation in the acrylic glass.

6.2 Measurements

6.2.1 CTC using operational measurements - Shift of reference planes

Plane i uses the amplifier signal, plane ii and iii the microphone directly at the loudspeaker. This means, that the sound radiated by the exciters and secondary sound radiated by the acrylic plates have almost no influence, similar to just the loudspeaker being used. On the other hand, the microphone in the channel measures also the secondary sound from the exciters, resulting in a higher level and such a higher contribution from sound in air in the planes iiC and iv.

So it can be said that all reference planes can be calculated more or less correctly when it comes to airborne sound. It just has to be taken care which sources can be measured at each point.

With the used sensors, reference plane iv is the only one able to determine the contribution from the bars separately, while plane i is not able to be combined with hammer measurements as the input was used differently. In addition to that plane ii and iii show the very similar results, the following investigations will only be performed for the planes iiC and iv. This is still enough to see the influence on hammer points before, at and after the reference plane. Additionally, the same physical modification measurement can be used as reference for all planes.

Table 5.3 and Figure B.2 indicate that the contribution by air can be synthesized well for the reference planes i, ii and iii if the comparison is made to only the loudspeaker being active, measurement S. Reference plane iv on the other hand fits well (when only the contribution in air is considered) for all sources, measurement T. Because of that, plane iiC was introduced, with the accelerometers from plane ii but the microphone in the connection channel.

6.2.2 CTC using Hammer measurements

6.2.2.1 Reference plane iiC

Table 5.4 shows an overestimation of the total sound pressure level in the receiving box. This can be attributed to the strong overestimation of the airborne sound. A possible explanation for this is the reflection from my body during the hammer measurements that could not be avoided and that a person in an anechoic chamber always increases the SPL in the room. Another possibility is the changed source location of airborne sound, as the hammer impacts were around the exciters and the loudspeaker for the measurements was in an adjacent corner. It also has to be mentioned that the hard plastic cap of the hammer resulted in a high-pitched noise when hitting the metal parts, which might explain the overestimation of the airborne sound at high frequencies that can be seen in Figure B.3. Therefore, using only Hammer measurements to perform a CTC should not be considered for usual applications, especially if airborne sound has to be included.

Nonetheless it is to be noted, that the overestimation results only for the first two groups of impact points from the contribution in air, while the structure-borne sound dominates in H3.

The overestimation of structure-borne sound in H3 results from a strong increase at high frequencies as it can be seen in Figure B.3. This can be explained by the frequency dependency of damping. The loss factor η is defined as the ratio between lost energy per period and reversible energy [15].

$$\eta = \frac{E_{\text{loss}}}{2\pi E_{\text{reversible}}} \tag{6.1}$$

As the period at high frequencies is shorter, more energy is lost on the way from the excitation point to both the answer point and the reference point. If the energy is induced in the transfer path, the transmissibility might be calculated with less energy at high frequencies at the reference point than at the answer point, leading to unphysical results. Even if the material damping in the path to the reference is lower than to the answer point, the measurement will be wrong and especially high frequencies will be overestimated.

A combination of all impact measurements is mostly dominated by the high levels obtained by H3 and results in levels with high deviation from real measurements.

6.2.2.2 Reference plane iv

If the transmissibilities are calculated for the reference plane iv, so for the physical separation plane, the overestimation by using only impulse hammer measurements of each path and also for the total SPL is much lower. Additionally, each impact point group is able to show if a path contributes more or less than any other. The 1/3 octave bands in Figure B.4 are showing an underestimation of low frequencies, while the high frequencies can be determined well. As the connection bars are hollow rectangular pipes and the excitation happened not on the same side as the sensor was mounted, this effect is also to be attributed to the frequency dependency of damping.

6.2.3 Combination of operational and impulse hammer measurements

6.2.3.1 Reference plane iiC

The reference plane iiC was able to separate well between the contribution from airborne and structure-borne sound when operational data were used. Also the total sound pressure level in the receiving box could be calculated with an acceptable accuracy.

When only impulse hammer measurements were used, the contribution by air was always overestimated, mostly at higher frequencies. The contribution by the structure was calculated too low when the impact point was far away from the answer point or drastically overestimated above 500 Hz if the hammer was used between the reference and the answer point.

The syntheses with a combined hammer and operational excitation result in a higher deviation from the measured data than the TPS performed with only operational data as it can be seen in Figure B.5. The overestimation in the airborne sound seen in subsubsection 6.2.2.1 for the first two hammer points, leading to a too high total level, is corrected to a more correct contribution. But the underestimation of the structure-borne sound seems to be dominant compared to the purely operational synthesis. The combination leads to an underestimation of the total level at the answer point.

The overestimation of all paths for the third hammer impact location is also passed on to the combined synthesis, leading to an overestimation of the total level.

Combining the operational measurements with all hammer impacts leads to a combination of two effects: the almost similar values of airborne and structure-borne contributions are mixed with the overestimated total level, resulting in too high levels in all three points.

6.2.3.2 Reference plane iv

The reference plane iv is the only one that is able to show all connections separately. In a synthesis performed with only operational data, the contribution of airborne sound was calculated correctly as a single value, and also the 1/3 octaves bands values in Figure B.2 match well. The total structure-borne sound contribution is slightly overestimated even if the contribution from bar 3 is underestimated.

The synthesis performed with only hammer measurements showed a good correspondence to the measurements, especially for the whole system. For the separate paths an overestimation towards high frequencies and an underestimation in low frequencies has to be noted.

When hammer and operational measurements are used together, each path can be determined well, especially if more information is available. The level for the whole system shows a slight deviation in some frequency bands (see Figure B.6), but the frequency development can be reproduced correctly. The contribution of airborne sound also shows a similar development, especially the hammer position on the exciters improves the calculation.

6.2.3.3 Amount of impulse hammer impacts

If only a single impulse hammer impact per location is added to the calculations, the contribution of bar 3, that couldn't be calculated correctly with a pure OTPA, increases to an almost correct total value. The 1/3 octave values in Figure B.7 reveal, that the deviation between the amounts of impacts is smaller than the deviation from the measurement. It can be said that a single impulse hammer hit per connection is already sufficient. In practice, at least 3 impact measurements should be performed as in a real setup the path is usually not as well accessible and to exclude measurement errors.

The contribution of all paths is hardly affected by the variation of impulse hammer impact points. The contribution of airborne sound is overestimated as soon as an impulse hammer is included, which can be deduced to the study shown in subsubsection 6.2.2.2. But with decreasing number of impact points, this deviation decreases.

6.2.3.4 Necessity of impacts on all paths

The same can be said about the total calculated structure-borne noise contribution and the overestimation of the influence of the bars 1 and 2. The contribution of bar 3 on the other hand can only be calculated correctly if all bars are excited by the impulse hammer, and also the deviation to the measured influence is the smallest in most frequency bands if every connection is included. This can be seen in Figure B.8. The best results can be reached for the contribution, if all bars are excited in both y and z directions.

6.2.4 Mesurement Rules

This thesis leads to the conclusion, that in case of inadequate excitation of the structure of interest an improvement of the contribution of each path can be reached by artificial excitation. A few things have to be considered if one wants to do so:

- The artificial excitation with an impulse hammer has to happen on all paths of the reference plane in as many directions as possible.
- One impact is sufficient, but more will increase the accuracy to a certain extend.
- If the reference plane considers more paths it can show a better compliance to the measurement than a reference plane close to the source.
- Artificial excitation should be performed either directly on the source if the signal is not sufficient to excite all frequencies, or on each path close to the indicator sensors if a path contribution is not calculated correctly. Excitation anywhere in between didn't bring any profit in the measurements performed for this thesis, excitation after the indicators resulted in wrong transmissibilities.
- For the Müller-BBM PAK Measurement system it has to be taken care that the channel names for both hammer measurements and operational measurements are identical. Additionally, for both, the frequency dependent data has to be saved.

If these few things are respected it is to be assumed that artificial excitation improves the result of an Operational Transfer Path Analysis.

7
Conclusion

In this thesis, the history and theory of transfer path analysis was shortly explained and recent developments especially in the OTPA were concluded.

A setup was developed to have a basis for transfer path measurements, in which all paths can be removed and investigated separately. The model consists of acrylic glass plates connected with aluminium bars for structure-borne sound transfer and wooden boxes with a channel for airborne sound. Special focus had to be laid upon the excitation of structure-borne noise as two commercial exciters, combined, should be used to excite the structure. Secondary airborne noise, radiated by either the exciters themselves or the acrylic glass plates in the sending box was used together with a loudspeaker for airborne noise excitation.

For each path of the setup, a contribution to the total sound pressure level in the receiving box could be derived and the reproducibility of measurements could be proved between 1 kHz and 5 kHz. Therefore, only the 1/3 octave bands in this region were used for further investigation.

Five reference planes could be found and all of them could be used well for an operational transfer path analysis and synthesis. It is shown that a crosstalk cancellation performed with a reference microphone very close to the loudspeaker leads to a good compliance in the synthesis to measurements with just the loudspeaker active, while a microphone in the airborne channel could be used to determine the total airborne sound contribution of all sources.

If the crosstalk cancellation was performed with only impulse hammer measurements the airborne sound contribution was almost always overestimated. For structure-borne sound excitation as close as possible to the reference plane has to be chosen for a relative path contribution allocation, but the levels cannot be assessed correctly.

A combination of excitation with an impulse hammer and operational data for the crosstalk cancellation lead to correct results of the synthesis of airborne sound if the reference plane was close to the source. The structure-borne sound could not be calculated correctly in this case. With a reference plane in the middle of the two boxes all path contributions could be determined correctly if the impulse hammer was used in the same plane. Impact points close to the source were not able to determine the contributions from both structure-borne sound connections correctly.

Artificial excitation in combination with operational data seems to help to determine the individual path contribution if the reference plane is not too close to the source and if the artificial excitation occurs close to the reference sensors.

If each path is excited by an impulse hammer directly, less flanking paths are excited and therefore the CTC has less influence on the result. But special attention should be paid to avoid exciting the path after the sensor, as this can lead to miscalculation due to the frequency dependency of internal losses.

If the excitation signal of the source is strongly coherent, an artificial excitation of the source itself can bring an improvement of the OTPA. This will also not do any harm to the measurement results.

If uncertainties exist if the hammer measurement were performed correctly it can be tried to use the same measurement for both the CTC and as source of the TPS. If the result at the answer of all paths varies substantially in the TPS, the hammer measurements should not be used.

Further investigation is necessary to verify these results in real applications like a car. This can be done by applying reference sensors close to the source and on each path. If artificial excitation before the source and on each path leads to similar deviations from the pure OTPA, this methodology can be said to be an improvement to the OTPA and also help to determine the path contribution if the operational signal is not sufficient to specify all frequencies or all paths.

Bibliography

[1] Tobias Kellert, Oliver Strauch, and Roland Sottek. Das Schallfeld in einem Kfz-Motorraum - Vergleich zwischen Messung und Simulation an einem vereinfachten 1:2-Modell. In *Fortschritte der Akustik : DAGA 03 ; [Plenarvorträge und Fachbeiträge der 29. Jahrestagung für Akustik DAGA 03, Aachen] / [Veranst.:] Rheinisch-Westfälische Technische Hochschule Aachen, RWTH. [Hrsg. des Tagungsbd.: Gottfried K. Behler]. - Bd. 1*, volume 29,1 of *Fortschritte der Akustik*, pages 288–289, Oldenburg, 2003. Dt. Ges. für Akustik (DEGA). Buch, CD-ROM.

[2] Herman Van der Auweraer, Peter Gajdatsy, Karl Janssens, Peter Mas, and Ludo Gielen. Innovative approaches to fast transfer path analysis. In M.M. Boone, editor, *Proceedings of the International Conference on Acoustics NAG/DAGA 2009*, pages 764–767. DEGA e.V., Berlin, 2009.

[3] Maarten V. van der Seijs, Dennis de Klerk, and Daniel J. Rixen. General framework for transfer path analysis: History, theory and classification of techniques. *Mechanical Systems and Signal Processing*, 68-69:217 – 244, 2016.

[4] J.W. Verheij. Measuring sound transfer through resilient mountings for separate excitation with orthogonal translations and rotations. *INTER-NOISE and NOISE-CON Congress and Conference Proceedings*, 1980(2), 1980.

[5] F.X. Magrans. Method of measuring transmission paths. *Journal of Sound and Vibration*, 74(3):321 – 330, 1981.

[6] K. Noumura and J. Yoshida. Method of transfer path analysis for vehicle interior sound with no excitation experiment. *FISITA WORLD AUTOMOTIVE CONGRESS -PROCEEDINGS- CD ROM EDITION-*, page F2206D183, 2006.

[7] J.M. Mondot and B. Petersson. Characterization of structure-borne sound sources: The source descriptor and the coupling function. *Journal of Sound and Vibration*, 114(3):507 – 518, 1987.

[8] N.B. Roozen and Q. Leclère. On the use of artificial excitation in operational transfer path analysis. *Applied Acoustics*, 74(10):1167 – 1174, 2013.

[9] Jakob Putner, Hugo Fastl, Martin Lohrmann, and Albert Kaltenhauser. Operational transfer path analysis predicting contributions to the vehicle interior noise for different excitations from the same sound source. 2012. `"https://mediatum.ub.tum.de/doc/1137875/477556.pdf"` visited: 2019-04-08.

[10] Wolfgang Ahnert and Hans-Peter Tennhardt. *Raumakustik*, pages 181–266. Springer Berlin Heidelberg, Berlin, Heidelberg, 2008.

[11] Christoph Kling. *Investigations into Damping in Building Acoustics by Use of Downscaled Models*. Dissertation, RWTH Aachen, 2008.

[12] Alexander Lee and Kurt Heutschi. Sound field estimation in courtyards. 2016. "https://www.ingentaconnect.com/content/ince(incecp/2016/00000253/00000006/art00042" visited: 2019-03-06.

[13] Tobias Kellert, Oliver Strauch, and Roland Sottek. Das Schallfeld in einem Kfz-Motorraum - Vergleich zwischen Messung und Simulation an einem vereinfachten 1:2-Modell. 2003. "http://publications.rwth-aachen.de/record/113716" visited: 2019-03-06.

[14] M. Möser. *Technische Akustik*. VDI-Buch. Springer Berlin Heidelberg, 2015.

[15] L. Cremer, M. Möser, W. Kropp, and M. Heckl. *Körperschall: Physikalische Grundlagen und technische Anwendungen*. Springer Berlin Heidelberg, 2009.

A

Appendix 1: Measurement Equipment

No	Location	Direction	Pos X in m	Pos Y in m	Pos Z in m
1.1	On Exciter Y	+X	0.06	0.43	0.07
1.2	On Exciter Y	-Y	0.1	0.45	0.07
1.3	On Exciter Y	+Z	0.1	0.43	0.12
1.4	On Exciter Z	+X	0.06	0.36	0.06
1.5	On Exciter Z	+Y	0.1	0.33	0.06
1.6	On Exciter Z	+Z	0.1	0.36	0.08
2.1	On Mount Southwest	+X	0.07	0.4	0.03
2.2	On Mount Southwest	+Z	0.07	0.4	0.04
2.3	On Mount Northwest	-X	0.13	0.4	0.03
2.4	On Mount East	+Y	0.1	0.34	0.03
3.1	On Bar 1	-Y	0.36	0.41	-0.02
3.2	On Bar 1	+Z	0.39	0.40	-0.01
3.3	On Bar 2	+Y	0.39	0.35	-0.02
3.4	On Bar 2	+Z	0.39	0.36	-0.01
3.5	On Bar 3	-Y	0.39	-0.03	0.1
3.6	On Bar 3	+Z	0.39	-0.02	0.11

Table A.1: Position and direction of all impulse hammer points.

No	Location	Direction	Pos X in m	Pos Y in m	Pos Z in m	Calibration difference in %
1	Exciter Y	-Y	0.13	0.41	0.07	-0.3
2	Exciter Z	-Z	0.13	0.34	0.04	-0.56
3	Amplifier	S	0	0	0	+3.99
4	Before Bearing	-X	0.07	0.38	0.03	-0.22
5	Before Bearing	+Z	0.07	0.38	0.03	-0.04
6	Before Bearing	+Y	0.07	0.38	0.03	0.03
7	After Bearing	-X	0.07	0.38	0	-0.02
8	After Bearing	+Z	0.07	0.38	0	0.04
9	After Bearing	-Y	0.07	0.38	0	0.22
10	Bar 1	-Z	0.39	0.41	-0.02	0.8
11	Bar 1	-Y	0.39	0.41	-0.02	-0.36
12	Bar 1	-X	0.39	0.41	-0.02	0.51
13	Bar 2	-Z	0.39	0.37	-0.02	0.45
14	Bar 2	-Y	0.39	0.37	-0.02	0.15
15	Bar 2	-X	0.39	0.37	-0.02	-0.10
16	Bar 3	-Z	0.39	-0.01	0.1	0.32
17	Bar 3	-Y	0.39	-0.01	0.1	0.04
18	Bar 3	-X	0.39	-0.01	0.1	-0.03
19	Receiving Point	-X	0.74	0.15	0	1.19
20	Receiving Point	+Z	0.74	0.15	0	0.51
21	Receiving Point	+Y	0.74	0.15	0	0.59
22	Source box	S	0.08	0.11	0.17	-0.90
23	Channel	S	0.41	0.22	0.26	0.17
24	Receiving box	S	0.74	0.15	0.24	-0.21

Table A.2: Position and calibration of all sensors in use for the measurements.

Sensor type	Channel	Brand	Model	Serial Number
Monoaxial accelerometer	1	Brüel & Kjær	4507C	30070
		Brüel & Kjær	2647A	2714078
Monoaxial accelerometer	2	Brüel & Kjær	4507C	30092
		Brüel & Kjær	2647A	2714079
Impulse Hammer	3	Brüel & Kjær	8202	1461449
		Brüel & Kjær	8200	unknown
Triaxial accelerometer	4:6	PCB	356A15	74018
Triaxial accelerometer	7:9	PCB	356A15	74019
Triaxial accelerometer	10:12	PCB	356A15	74685
Triaxial accelerometer	13:15	PCB	356A15	79321
Triaxial accelerometer	16:18	PCB	356A15	79322
Triaxial accelerometer	19:21	PCB	356A15	93883
Microphone	22	PCB	378B02	10367
Microphone	23	PCB	378B02	LW111128
Microphone	24	PCB	378B02	135494
Calibrator accelerometers		Brüel & Kjær	4294	2849607
Calibrator microphones		Brüel & Kjær	4230	1025957
Measurement System MKII by Müller-BBM VAS				
			PQ20 G2	1114M1309
	1:16		SC42	1008M5139
	17:24		SC42S7	0712M1741
	1:4		ICP422	1007M9645
	5:8		ICP422	0906M3811
	9:12		ICP422	1007M9635
	13:16		ICP429	0910M0260
	17:20		ICP429	0910M0357
	21:24		ICP422	0806M3134

Table A.3: Measurement hardware used for all measurements.

B

Appendix 2: 1/3 octave levels

B.1 Physical modifications

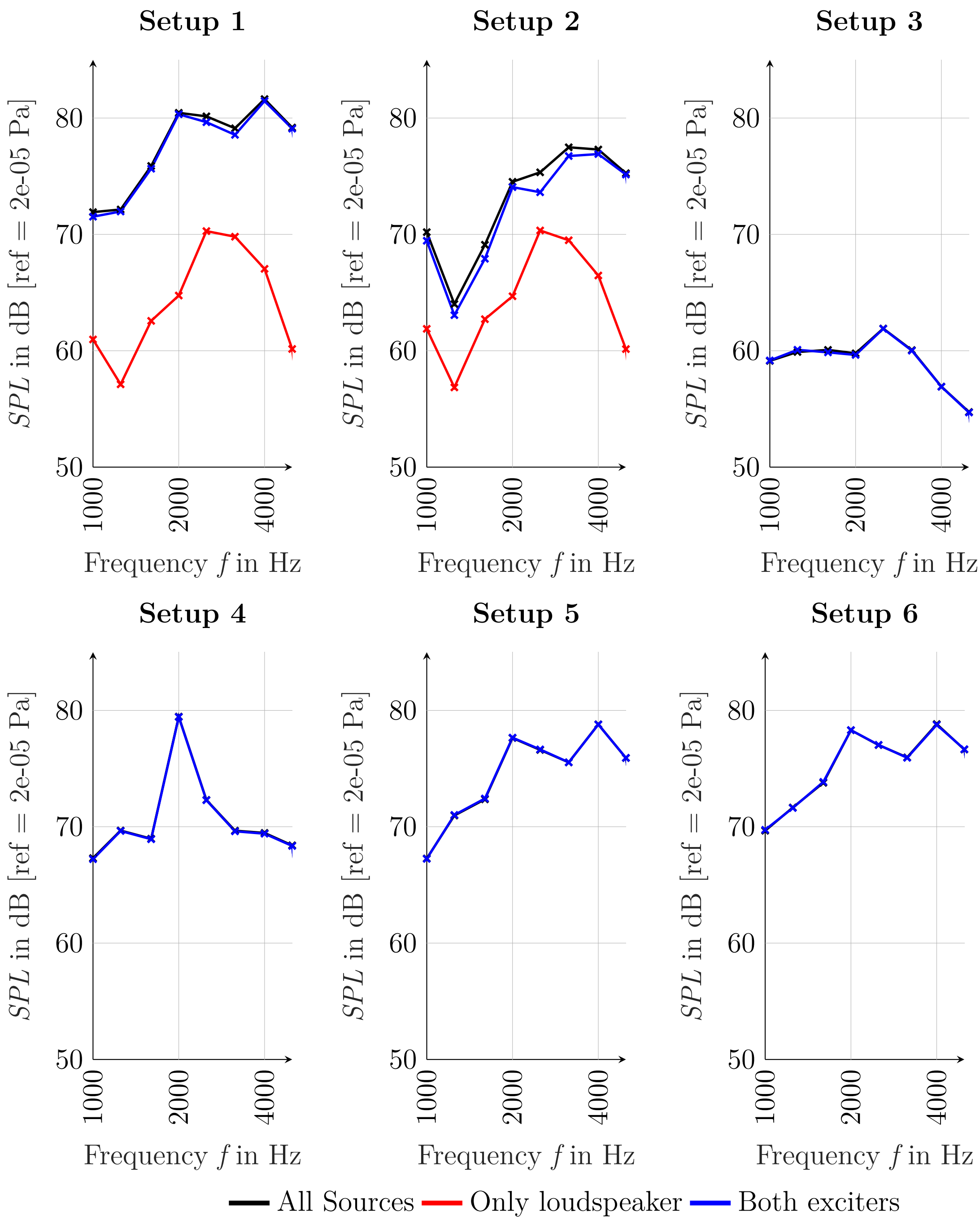

Figure B.1: Sound Pressure Level in the receiving box of the model with different settings of connections between the two boxes. The level from only the loudspeaker in the setups 3 to 6 is between 35 dB and 50 dB and therefore not plotted here.

B.2 Results

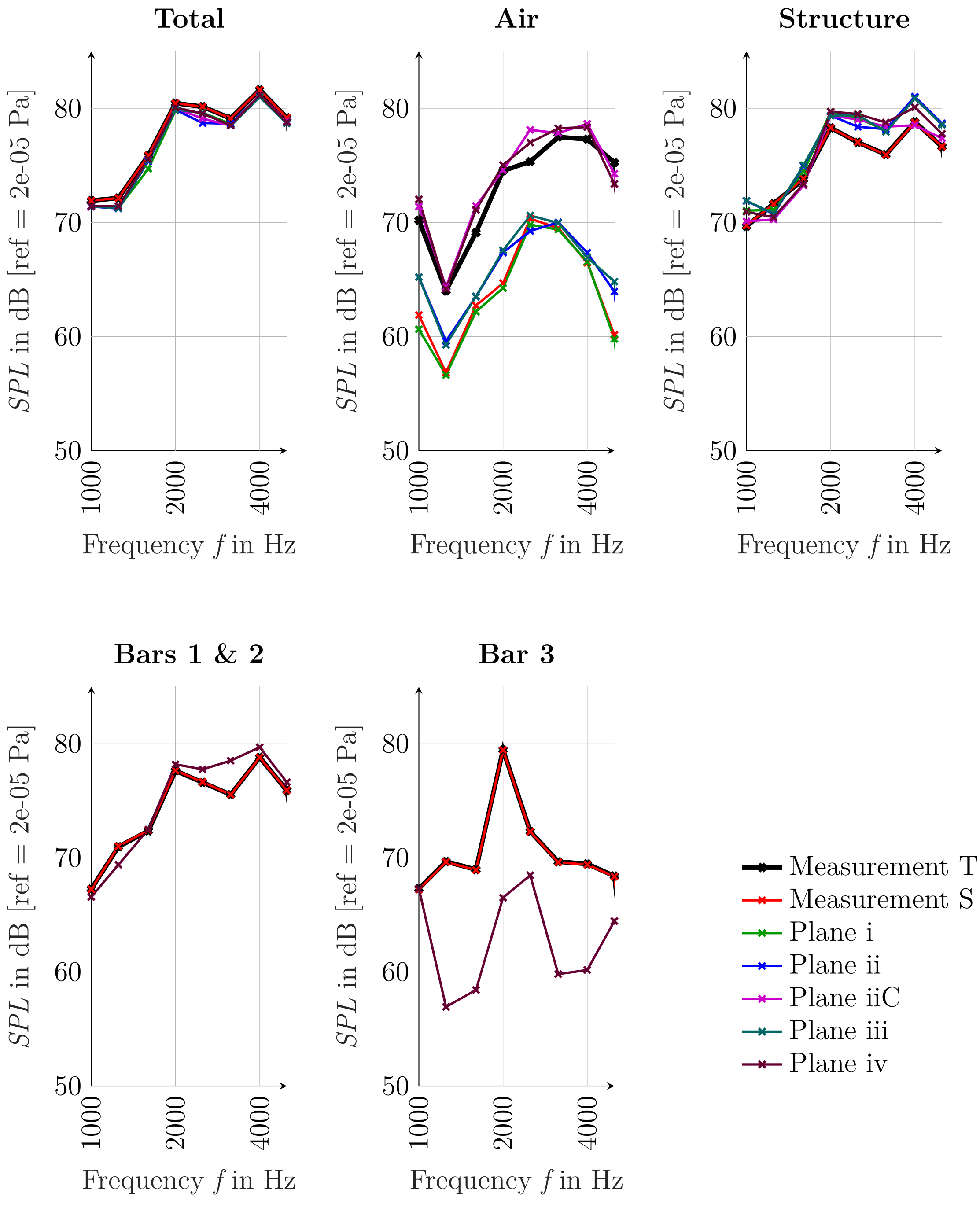

Figure B.2: Sound Pressure Level in the receiving box of the measurements and synthesis results without additional excitation on all reference planes.

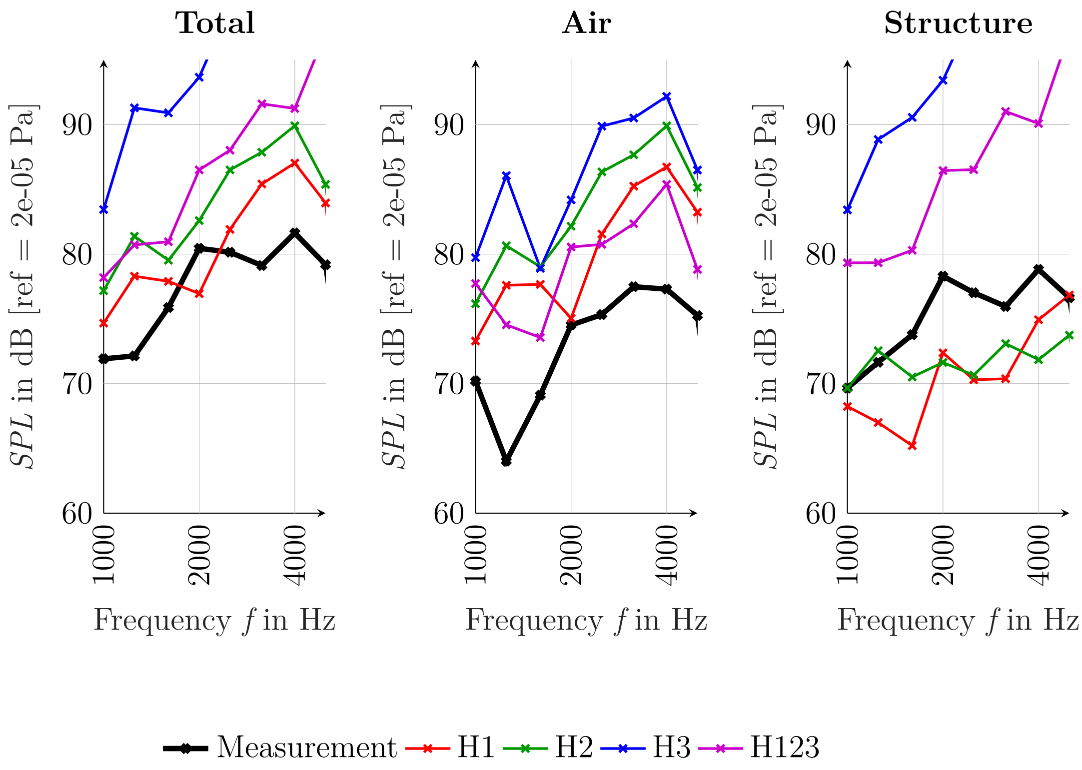

Figure B.3: Sound Pressure Level in the receiving box of the measurements and synthesis results with only hammer impacts in reference plane iiC.

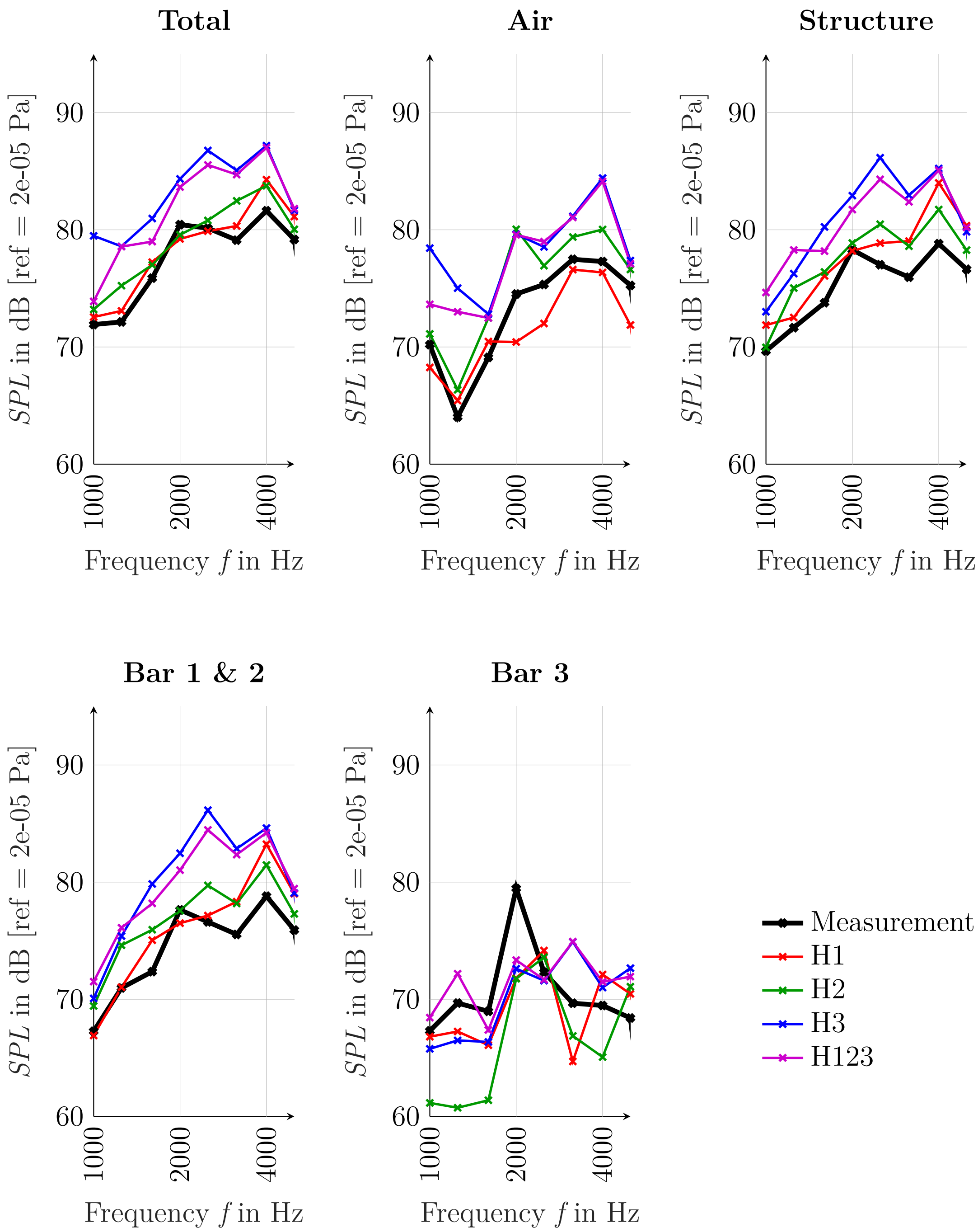

Figure B.4: Sound Pressure Level in the receiving box of the measurements and synthesis results with only hammer impacts in reference plane iv.

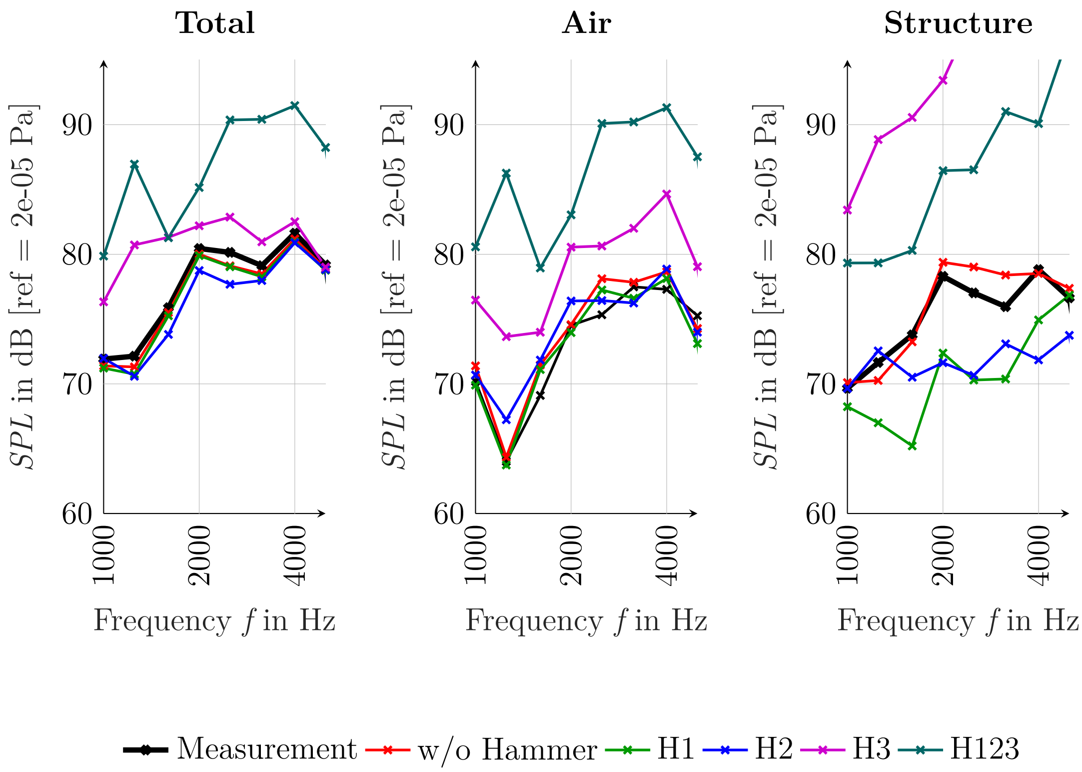

Figure B.5: Sound Pressure Level in the receiving box of the measurements and synthesis results with operational data and additional artificial excitation in reference plane iiC.

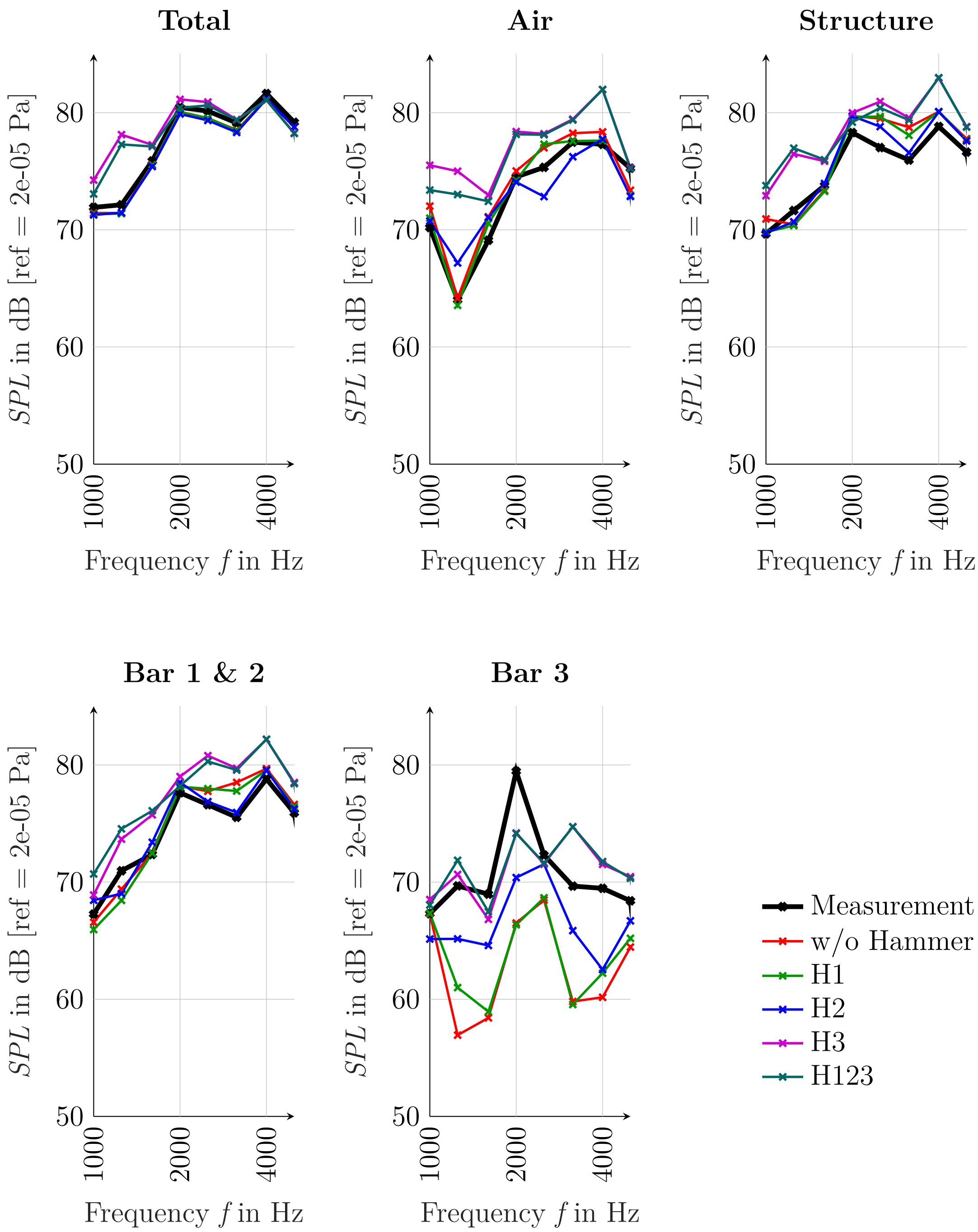

Figure B.6: Sound Pressure Level in the receiving box of the measurements and synthesis results with operational data and additional artificial excitation in reference plane iv.

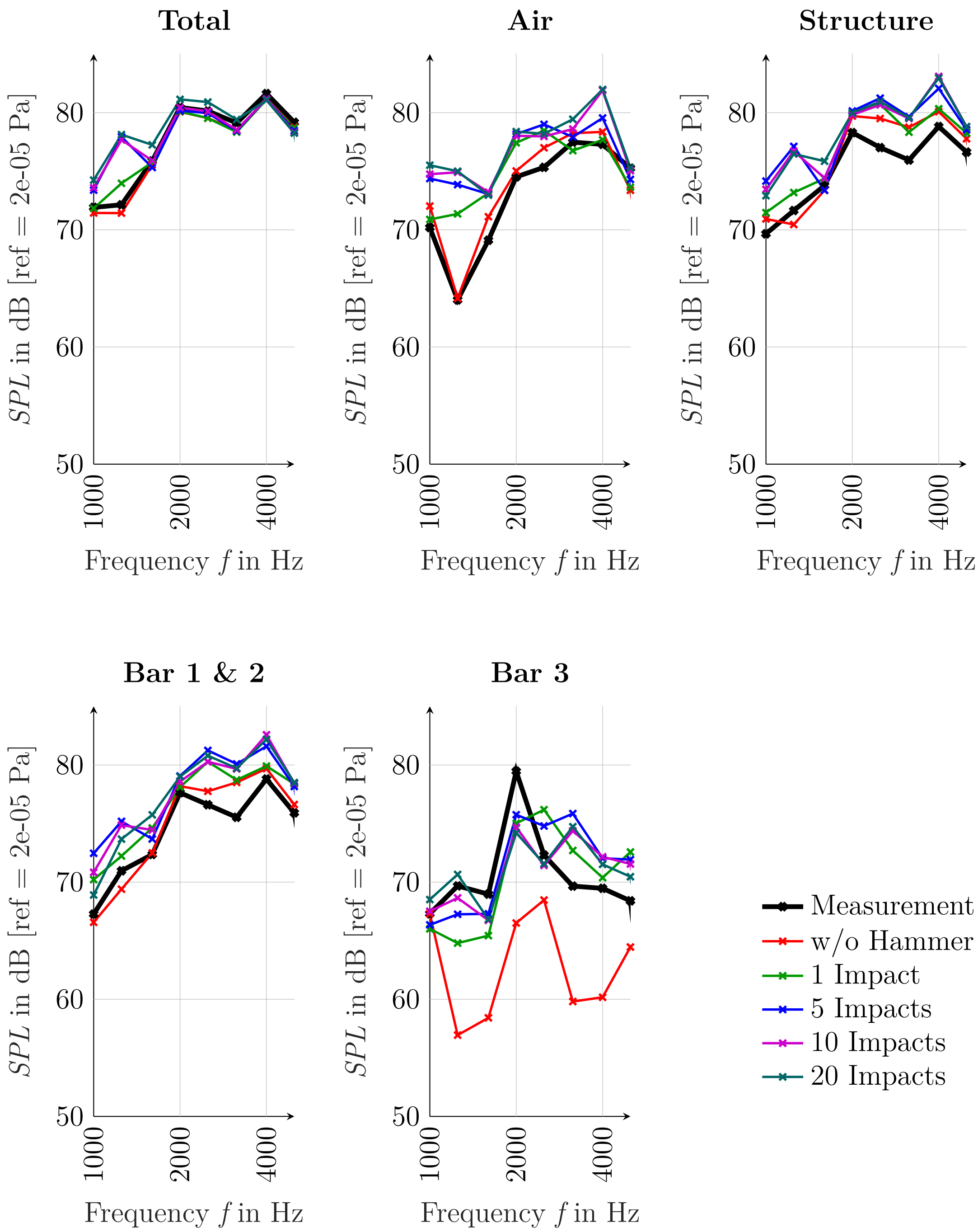

Figure B.7: Sound Pressure Level in the receiving box of the measurements and synthesis results with operational data and additional artificial excitation in reference plane iv with a different number of impulse hammer impacts.

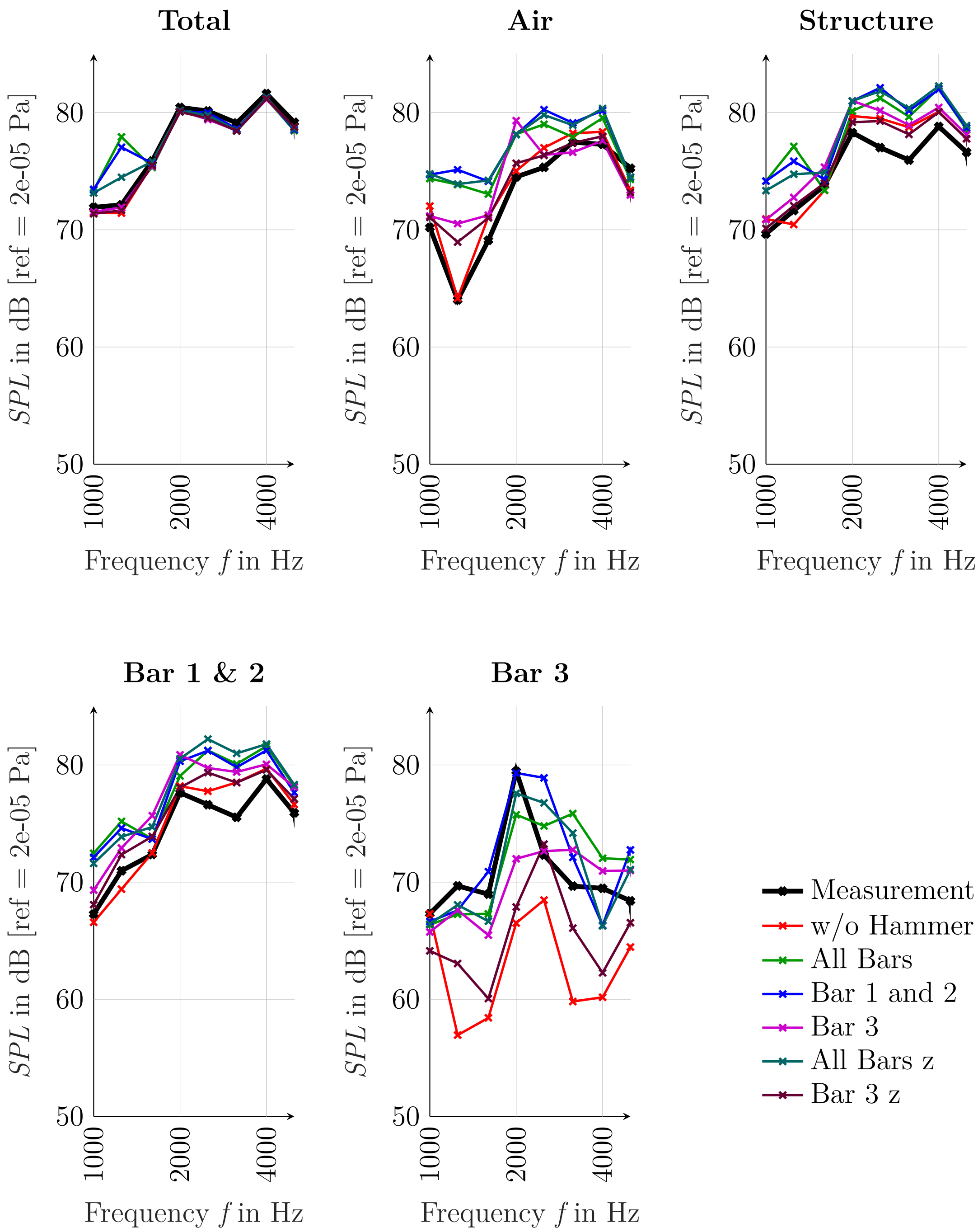

Figure B.8: Sound Pressure Level in the receiving box of the measurements and synthesis results with operational data and additional artificial excitation in reference plane iv with 5 impulse hammer impacts on different paths of the reference plane.